Mechanical Systems and Signal Processing ∎ (∎∎∎∎) ∎∎∎–∎∎∎

Contents lists available at ScienceDirect

Mechanical Systems and Signal Processing

journal homepage: www.elsevier.com/locate/ymssp

Finite element model updating using the shadow hybrid Monte Carlo technique

I. Boulkaibet [a,*], L. Mthembu [a], T. Marwala [a], M.I. Friswell [b], S. Adhikari [b]

[a] The Centre For Intelligent System Modelling (CISM), Electrical and Electronics Engineering Department, University of Johannesburg, PO Box 524, Auckland Park 2006, South Africa
[b] College of Engineering, Swansea University, Singleton Park, Swansea SA2 8PP, United Kingdom

ARTICLE INFO

Article history:
Received 25 December 2013
Received in revised form
19 May 2014
Accepted 11 June 2014

Keywords:
Bayesian
Sampling
Finite Element Model updating
Markov Chain Monte Carlo
Hybrid Monte Carlo method
Shadow Hybrid Monte Carlo

ABSTRACT

Recent research in the field of finite element model updating (FEM) advocates the adoption of Bayesian analysis techniques to dealing with the uncertainties associated with these models. However, Bayesian formulations require the evaluation of the Posterior Distribution Function which may not be available in analytical form. This is the case in FEM updating. In such cases sampling methods can provide good approximations of the Posterior distribution when implemented in the Bayesian context. Markov Chain Monte Carlo (MCMC) algorithms are the most popular sampling tools used to sample probability distributions. However, the efficiency of these algorithms is affected by the complexity of the systems (the size of the parameter space). The Hybrid Monte Carlo (HMC) offers a very important MCMC approach to dealing with higher-dimensional complex problems. The HMC uses the molecular dynamics (MD) steps as the global Monte Carlo (MC) moves to reach areas of high probability where the gradient of the log-density of the Posterior acts as a guide during the search process. However, the acceptance rate of HMC is sensitive to the system size as well as the time step used to evaluate the MD trajectory. To overcome this limitation we propose the use of the Shadow Hybrid Monte Carlo (SHMC) algorithm. The SHMC algorithm is a modified version of the Hybrid Monte Carlo (HMC) and designed to improve sampling for large-system sizes and time steps. This is done by sampling from a modified Hamiltonian function instead of the normal Hamiltonian function. In this paper, the efficiency and accuracy of the SHMC method is tested on the updating of two real structures; an unsymmetrical H-shaped beam structure and a GARTEUR SM-AG19 structure and is compared to the application of the HMC algorithm on the same structures.

1. Introduction

Finite element models (FEMs) are well-known numerical methods used to provide approximate solutions for complex engineering problems [1,2]. In mechanical engineering the FEM method is often used for computing displacements, stresses and strains in structures under a set of loads. However, FEM results degrade with an increase in problem complexity. The result is that the FEM results for the complex system differ from those obtained from experiments [3,4]. These differences can mainly be attributed to modeling errors, especially the uncertainties associated with modeling some structural feature

* Corresponding author.
E-mail address: ilyes@aims.ac.za (I. Boulkaibet).

http://dx.doi.org/10.1016/j.ymssp.2014.06.005
0888-3270/

(and properties as per manufacturing process) and or modeling the possible dynamics of those features. Therefore, the initial FE model needs to be updated to match the measured data. There are two main classes of model updating: direct method and the indirect (iterative) methods. The direct methods are computationally efficient approaches that update the FEM matrix components in one step [5,6]. However, high quality measurements as well as accurate FE models are required for this updating process. Using direct methods often results in unrealistic updating parameter values hence these parameters lose their physical meaning. On the other hand iterative FEM methods use cost functions to iteratively reduce the error between the experimental and analytical results. This is done by modifying (updating) the uncertain parameters in the modeled system [7]. The most common iterative approaches are the sensitivity-based updating methods see Link [8] for a review. In the last decade, the nature-inspired optimization algorithms have been widely applied in the area of model updating. These algorithms represent a class of probabilistic search algorithms that cope well with non-convex optimization problems. In these algorithms, controlled random steps are used during the searching procedure where the new search position is somehow based on the previous one. Levin et al. [9] applied the simulated annealing (SA) method and the genetic algorithm (GA) to update simulated and experimental systems while Marwala [4] used a Particle Swarm Optimization (PSO) algorithm to update a H-Beam structure.

Unfortunately, most of deterministic algorithms based on optimization do not quantify the involved uncertainties in structures tests. In the case of uncertain systems, the classical deterministic algorithms based on optimization do not quantify the involved uncertainties and this may degrade the accuracy of the obtained results. On the other hand, uncertainty quantification methods are designed to quantify uncertainties in engineering problems [4,7,10]. There are two main classes of uncertainty quantification methods: Probabilistic methods and non-probabilistic methods. Probabilistic methods such as Bayesian methods, perturbation methods are based on probability theory in which the uncertain parameters are modeled as random parameters. The interval arithmetic and the fuzzy methods belong to the non-probabilistic class [7].

In recent years Bayesian model updating techniques have shown promising results in systems identification type problems–of which FEM updating is one [4,11–13]. The Bayesian approach possesses the ability to characterize and quantify the uncertainties of a modeled system. This can be done by representing uncertain parameters as random vectors with a joint probability density function (PDF). This density function is known as the posterior distribution function. The use of Bayesian techniques becomes useful when an analytical solution to this function, the posterior, is not available. This is the case in FEM updating because of the high dimensional parameter search space.

Different methods have been proposed to estimate the PDF – the most common method being the maximum likelihood. This method represents an asymptotic approximation to the full Bayesian solution and it can be applied in the case where the unknown parameters are modeled as Gaussian. The most probable values are obtained by maximizing the likelihood function and the covariance matrix is obtained by using the Hessian of the likelihood function [9].

An alternative to the above is to use sampling techniques to estimate the PDF. Different methods such as Latin Hypercube Sampling (LHS) [14], Orthogonal Array Sampling [15] have been developed to predict complex distributions. The LHS method has been employed in model updating by Khodaparast [7]. Among sampling methods the most popular are the Markov chain Monte Carlo (MCMC) methods. These methods allow sampling from a large class of distributions and some of these algorithms cop well with the dimensionality of the sample space. The Metropolis–Hastings (MH) algorithm is the most common MCMC algorithm [16–19]. This method samples from a proposed PDF and the acceptance-rejection step is used to ensure that the Markov chain is reversible with respect to the stationary target density function [19]. The proposed PDF used to generate the samples forms a random walk trajectory during the search. In the MH algorithm smaller transitions can assure a high acceptance rate but a large amount of time is needed to cover more space during the search procedure. The random walk step becomes useless for complex systems where highly correlated samples can be obtained with a poor mixing of the chain and the MH acceptance rate will decrease exponentially. The MH algorithm has been implemented on the FEM updating problem [4,12,20].

Ching et al. [21] successfully applied another MC method called Gibbs sampling [22] to solve high-dimensional model updating problems. Based on the MH algorithm, Ching and Cheng [23] introduced the Transitional Markov Chain Monte Carlo (TMCMC) algorithm and Muto and Beck [24] applied it to the updating of hysteretic structural models. Cheung and Beck [11] applied the Hybrid Monte Carlo (HMC) method to update a linear structural dynamic model with 31 uncertain parameters. The probabilistic Bayesian model updating approach used in [11] was able to characterize modeling uncertainties associated with the underlying structural system. The HMC method promises the ability to solve higher-dimensional complex problems. The Monte Carlo trajectory it uses is guided by the derivative of the target log-density probability which leads towards areas of high probability during the searching process [25]. In this method the updated parameter vector is treated as a system displacement and an auxiliary variable, called the momentum vector, is introduced to construct a new Molecular Dynamic (MD) system. The total system energy – called the Hamiltonian function – is evaluated using the Störmer-Verlet (also called leapfrog integrator) algorithm. However, the Störmer–Verlet integrator does not conserve energy especially when the time step used and/or the system size are considered large. To overcome this limitation, a modified HMC algorithm called the Shadow Hybrid Monte Carlo (SHMC) was proposed in [26].

In this paper the SHMC is implemented for its proposed good-ability to sample the posterior PDF. This method is tested on updating FE models of an unsymmetrical H-shaped Structure and the GARTEUR SM-AG19 structure. The accuracy, efficiency and limitations of the SHMC technique are compared to those of the HMC algorithm on the same structures.

In the next section a short theoretical background of finite element model is presented. In Section 3 the posterior distribution function of the uncertain parameters of the FEM are presented. Section 4 introduces the HMC technique.

Please cite this article as: I. Boulkaibet, et al., Finite element model updating using the shadow hybrid Monte Carlo technique, Mech. Syst. Signal Process. (2014), http://dx.doi.org/10.1016/j.ymssp.2014.06.005

Section 5 introduces the SHMC technique which is used to predict the Posterior PDF of the FEM updating parameters. Section 6 presents the construction of the Shadow Hamiltonian function. Section 7 presents an implementation of Bayesian FEM updating on an unsymmetrical H-shaped Structure. Section 8 presents the second implementation of the Bayesian FEM updating on the GARTEUR SM-AG19 structure. Section 9 concludes the paper.

2. Finite element model background

In finite element modeling, an N degree of freedom dynamic structure may be described by the matrix equation of motion [12,29,30]:

$$\mathbf{M}\ddot{\mathbf{x}}(t)+\mathbf{C}\dot{\mathbf{x}}(t)+\mathbf{K}\mathbf{x}(t)=\mathbf{f}(t), \tag{1}$$

where $\mathbf{M}$,$\mathbf{C}$ and $\mathbf{K}$ are the mass, damping and stiffness matrices of size $N\times N$, $\mathbf{x}(t)$ is the vector of N degrees of freedom and $\mathbf{f}(t)$ is the vector of loads applied to the structure. In the case that no external forces are applied to the structure and if the damping terms are neglected (i.e. its influence is very small, $\mathbf{C}\sim\mathbf{0}$), the dynamic equation may be written in the modal domain (natural frequencies and mode shapes) where the error vector for the ith mode is obtained from:

$$(-(\omega_i^m)^2\mathbf{M}+\mathbf{K})\phi_i^m=\varepsilon_i \tag{2}$$

ω_i^m is the ith measured circular natural frequency ($\omega_i^m=2\pi f_i^m$ and f_i^m is the ith measured natural frequency), ϕ_i^m is the ith measured mode shape vector and ε_i is the ith error vector. In Eq. (2), the error vector ε_i is equal to $\mathbf{0}$ if the system matrices $\mathbf{M}$ and $\mathbf{K}$ correspond to the modal properties (ω_i^m and ϕ_i^m). However, ε_i is a non-zero vector if the system matrices obtained analytically from the finite element model do not match the measured modal properties ω_i^m and ϕ_i^m.

3. Bayesian Inference

In order to update the FE model the uncertain model (system) parameters have to be identified. This paper does not deal with identifying the uncertain parameters of a model but assumes they have a prior been identified. The identification of the uncertain parameters in a potential list of parameters is a feature selection problem [31,32,46]. Having obtained the uncertain parameters Bayesian inference can then be used to calculate their posterior distribution(s). Bayesian approaches are governed by Bayes [12,29,31] rule:

$$P(\boldsymbol{\theta}|D)\propto P(D|\boldsymbol{\theta})P(\boldsymbol{\theta}) \tag{3}$$

where $\boldsymbol{\theta}$ represent the vector of updating parameters and the mass $\mathbf{M}$ and stiffness $\mathbf{K}$ matrices are functions of the updating parameters $\boldsymbol{\theta}$ ($\mathbf{M}=\mathbf{M}(\boldsymbol{\theta})$ and $\mathbf{K}=\mathbf{K}(\boldsymbol{\theta})$). The D matrix is the measured modal properties (the natural frequencies f_i^m and mode shapes ϕ_i^m). The quantity $P(\boldsymbol{\theta})$ known as the prior probability distribution function, is a function of the updating parameters in the absence of the data D. The quantity $P(\boldsymbol{\theta}|D)$ is the posterior probability distribution function of the parameters in the presence of the data D. $P(D|\boldsymbol{\theta})$ is the likelihood function [4,20,31].

The likelihood function is the probability of the modal measurements in the presence of uncertain parameters. This function can be defined as the normalized exponent of the error function that represents the differences between the measured and the analytic modal properties (i.e. frequencies in Eq. 4):

$$P(D|\boldsymbol{\theta})=\frac{1}{((2\pi/\beta))^{N_m/2}\prod_{i=1}^{N_m}\omega_i^m}\exp\left(-\frac{\beta_c}{2}\sum_i^{N_m}\left(\frac{f_i^m-f_i}{f_i^m}\right)^2\right) \tag{4}$$

where β_c is a constant, N_m is the number of measured modes and $f_i=f_i(\boldsymbol{\theta})$ is the ith analytical frequency obtained from the FEM.

The prior function represents the prior knowledge about the updating parameters ($\boldsymbol{\theta}$). For structural system the prior knowledge could be the observation that parameters near joints should be updated more intensely than for those corresponding to smooth surface areas far from joints. The prior PDF for parameters $\boldsymbol{\theta}=(\theta_i,\ \ldots,\ \theta_Q)$ in Eq. 5 is assumed to be Gaussian and is given by [20,29,32]:

$$P(\boldsymbol{\theta})=\frac{1}{(2\pi)^{Q/2}\prod_{i=1}^{Q}(1/\sqrt{\alpha_i})}\exp\left(-\sum_i^Q\frac{\alpha_i}{2}\|\theta_i-\theta_i^0\|^2\right) \tag{5}$$

where Q is the number of parameters to be updated, $\boldsymbol{\theta}_0=(\theta_1^0,\ \ldots.,\theta_Q^0)$ represents the mean value of the updated vector and α_i is the coefficient of the prior PDF for the ith updated parameter. The notation $\|*\|$ denotes the Euclidean norm of *. If α_i is a constant for all the updating parameters in Eq. (5) then the updated parameters will be of the same order of magnitude. Eq. (5) may be viewed as a regularization parameter [12,20,33]. In Eq. (5) Gaussian priors are conveniently chosen because many natural processes tend to have a Gaussian distribution.

The posterior distribution function of the parameters $\boldsymbol{\theta}$ given the observed data D is denoted as $P(\boldsymbol{\theta}|D)$ and is obtained by applying Bayes' theorem as represented in Eq. (3). The distribution $P(\boldsymbol{\theta}|D)$ is calculated by substituting Eqs. (4) and (5) into

Please cite this article as: I. Boulkaibet, et al., Finite element model updating using the shadow hybrid Monte Carlo technique, Mech. Syst. Signal Process. (2014), http://dx.doi.org/10.1016/j.ymssp.2014.06.005

Eq. (3) to give

$$P(\boldsymbol{\theta}|D) \propto \frac{1}{Z_s(\alpha,\beta)} \exp\left(-\frac{\beta_c}{2} \sum_{i}^{N_m} \left(\frac{f_i^m - f_i}{f_i^m} \right)^2 - \sum_{i}^{Q} \frac{\alpha_i}{2} \| \theta_i - \theta_i^0 \|^2 \right) \tag{6}$$

Where

$$Z_s(\alpha,\beta) = \left(\frac{2\pi}{\beta} \right)^{N_m/2} \prod_{i=1}^{N_m} f_i^m (2\pi)^{Q/2} \prod_{i=1}^{Q} \frac{1}{\sqrt{\alpha_i}} \tag{7}$$

The Eq. (6) can be written in the following Normal distribution form:

$$P(\boldsymbol{\theta}|D) = \frac{1}{(2\pi)^{(N_m+Q/2)} |\Sigma|^{(1/2)}} exp\left(-\frac{1}{2} (\boldsymbol{X} - \boldsymbol{\mu})^T \Sigma^{-1} (\boldsymbol{X} - \boldsymbol{\mu}) \right) \tag{8}$$

Where

$$\boldsymbol{X} = [f_1, \ldots . f_{N_m}, \theta_1, \ldots., \theta_Q], \ \boldsymbol{\mu} = \left[f_1^m, \ \ldots . f_{N_m}^m, \theta_1^0, \ldots., \theta_Q^0 \right] \text{ and } \Sigma^{-1} = \begin{bmatrix} \frac{\beta_c}{f_1^{m2}} & 0 & \ldots & & & \\ 0 & \ddots & 0 & & 0 & \\ \vdots & 0 & \frac{\beta_c}{f_{Nm}^{m2}} & & & \\ & & & \alpha_1 & 0 & \vdots \\ & 0 & & 0 & \ddots & 0 \\ & & & \ldots & 0 & \alpha_Q \end{bmatrix}$$

In most cases, the analytical form of the posterior PDF solution is not be available due the complexity of the system as well as the high dimensionality of the parameter search space. In these situations, the sampling methods provide the only practical solution to estimating this function. Sampling techniques can simplify the Bayesian inference by providing a set of random samples from the posterior distribution [11, 12, 20, 29, 31, 34]. If Y is the observation of certain parameters at different discrete time instants then the Total Probability theorem provides the probabilistic information for the prediction of the future responses Y at different time instants. Consider the following integral;

$$P(Y|D) = \int P(Y|\boldsymbol{\theta}) P(\boldsymbol{\theta}|D) d\boldsymbol{\theta} \tag{9}$$

Eq. (9) depends on the posterior distribution function. The dimension of the updating parameters and the complexity of the modeled system make it very difficult to obtain an analytical solution. Therefore, sampling techniques, such as Markov chain Monte Carlo (MCMC) methods are employed to predict the updating parameter distribution and subsequently to predict the modal properties. Given a set of N_s random parameter vectors drawn from a PDF $P(\boldsymbol{\theta}|D)$, the expectation value of any observed function Y can be easily estimated.

The integral in Eq. (9) can be solved using sampling algorithms [11,31,35,36]. These algorithms are used to generate a sequence of vectors $\{\boldsymbol{\theta}_1, \boldsymbol{\theta}_2, \ldots, \boldsymbol{\theta}_{N_s}\}$ where N_s is the number of samples and these vectors can be used to form a Markov chain. This generated vector is then used to predict the form of the posterior distribution function$P(\boldsymbol{\theta}|D)$. The integral in Eq. (9) can be approximated as

$$\tilde{Y} \cong \frac{1}{N_s} \sum_{i=1}^{N_s} G(\boldsymbol{\theta}_i) \tag{10}$$

where G is a function that depends on the updated parameters $\boldsymbol{\theta}_i$. As an example, if $\mathbf{G}=\boldsymbol{\theta}$ then $\tilde{Y}$ becomes the expected value of $\boldsymbol{\theta}$. Generally, $\tilde{Y}$ is the vector that contains the modal properties and N_s is the number of retained states. In this paper, the HMC and the SHMC methods are used to sample from the posterior PDF.

4. The Hybrid Monte Carlo (HMC) method

The Hybrid Monte Carlo method, known as the Hamiltonian Monte Carlo method, is a method for solving higher-dimensional complex problems [11,25,29,31,36]. The HMC combines a Molecular Dynamic (MD) trajectory with a Monte Carlo (MC) rejection step [12]. In HMC, a dynamical system is considered in which auxiliary variables, called momentum, $\mathbf{p} \in R^N$, are introduced. The updated vector $\boldsymbol{\theta}$ is treated as displacements. The total energy (Hamiltonian function) of the new dynamical system is defined by $H(\boldsymbol{\theta}, \mathbf{p}) = V(\boldsymbol{\theta}) + W(\mathbf{p})$, where the potential energy is defined by $V(\boldsymbol{\theta}) = -\ln(P(\boldsymbol{\theta}|D))$ and the kinetic energy $W(\mathbf{p}) = \mathbf{p}^{\mathbf{T}} \mathbf{M}^{-1} \mathbf{p}/2$ depends only on $\mathbf{p}$ and some chosen positive definite matrix $\mathbf{M} \in R^{N \times N}$.

The Hamiltonian dynamics associated with $H(\boldsymbol{\theta}, \mathbf{p})$ are governed by:

$$\frac{d\boldsymbol{\theta}}{dt} = \mathbf{M}^{-1} \mathbf{p}(t), \ \frac{d\boldsymbol{p}}{dt} = -\nabla V(\boldsymbol{\theta}(t)) \tag{11}$$

Please cite this article as: I. Boulkaibet, et al., Finite element model updating using the shadow hybrid Monte Carlo technique, Mech. Syst. Signal Process. (2014), http://dx.doi.org/10.1016/j.ymssp.2014.06.005

In this paper, Molecular Dynamic simulations are performed under the conditions of constant temperature T, constant volume V, and constant number of particles N (canonical ensemble). The density function $\rho(\boldsymbol{\theta},\mathbf{p})$ of the canonical ensemble follows a Boltzmann distribution. This ensemble is believed to be good representation of the distribution of the Hamiltonian system if it is in thermal contact with a much larger system of temperature T. A nice feature of this ensemble is that position $\boldsymbol{\theta}$ and momentum $\mathbf{p}$ are independent for separable Hamiltonians [37].

The joint distribution derived from the Hamiltonian function can be written as: $\rho(\boldsymbol{\theta},\mathbf{p}) \propto \exp(-\beta_B H(\boldsymbol{\theta},\mathbf{p}))$ where $\beta_B = (1/K_B T)$ and K_B is a Boltzmann constant and T is temperature. It is easy to see that $\rho(\boldsymbol{\theta},\mathbf{p})$ can be rewritten as $\rho(\boldsymbol{\theta},\mathbf{p}) \propto \exp(-\beta_B V(\boldsymbol{\theta})).\exp(-\beta_B W(\mathbf{p}))$ or $\rho(\boldsymbol{\theta},\mathbf{p}) \propto P(\boldsymbol{\theta}|D).\exp(-\beta_B \mathbf{p}^{\mathbf{T}}\mathbf{M}^{-1}\mathbf{p}/2)$. Clearly, sampling $\boldsymbol{\theta}$ from the posterior distribution can also be obtained by sampling $(\boldsymbol{\theta},\mathbf{p})$ from the joint distribution $\rho(\boldsymbol{\theta},\mathbf{p})$ where $\boldsymbol{\theta}$ and $\boldsymbol{p}$ are independent according to $H(\boldsymbol{\theta},\mathbf{p})$ (a separable Hamiltonian function).

The evolution of $(\boldsymbol{\theta},\mathbf{p})$ through time t can be numerically achieved by using the Störmer–Verlet or leapfrog scheme [11,12]

$$\mathbf{p}\left(t+\frac{\delta t}{2}\right) = \mathbf{p}(t) - \frac{\delta t}{2}\nabla V(\boldsymbol{\theta}(t)) \tag{12}$$

$$\boldsymbol{\theta}(t+\delta t) = \boldsymbol{\theta}(t) + \delta t \mathbf{M}^{-1}\mathbf{p}\left(t+\frac{\delta t}{2}\right) \tag{13}$$

$$\mathbf{p}(t+\delta t) = \mathbf{p}\left(t+\frac{\delta t}{2}\right) - \frac{\delta t}{2}\nabla V(\boldsymbol{\theta}(t+\delta t)) \tag{14}$$

where δt is the time step and ∇V is obtained numerically by finite differences as:

$$\frac{\partial V}{\partial \theta_i} = \frac{V(\boldsymbol{\theta}+\Delta h) - V(\boldsymbol{\theta}-\Delta h)}{2h\Delta_i} \tag{15}$$

$\Delta = [\Delta_1, \Delta_2, \ldots, \Delta_N]$is the perturbation vector and h is a scalar which dictates the size of the perturbation of $\boldsymbol{\theta}$.

In practice, the Störmer–Verlet algorithm does not preserve the property of Eq. (10), where the probability density function is proportional to $\exp(-\beta_B H(\boldsymbol{\theta},\mathbf{p}))$ [25]. In order to satisfy the property of Eq. (11), an accept–reject step must be added. In such a case, after each iteration of Eqs. (12)–(14), the resulting candidate state is accepted or rejected according to the Metropolis criterion based on the value of the Hamiltonian $H(\boldsymbol{\theta},\mathbf{p})$. Thus, if $(\boldsymbol{\theta},\ \mathbf{p})$ is the initial state and $(\boldsymbol{\theta}^*,\mathbf{p}^*)$ is the state after the equations above have been updated, then this candidate state is accepted with probability $\min(1,\ \exp\{-\beta_B \Delta H\})$, $\Delta H = H(\boldsymbol{\theta}^*,\mathbf{p}^*) - H(\boldsymbol{\theta},\mathbf{p})$. The obtained vector $\boldsymbol{\theta}^*$ will be used for the next iteration. The algorithm stopping criterion is defined by the number of $\boldsymbol{\theta}$ samples (N_s). The HMC algorithm can be summarized as follows:

1) A value $\boldsymbol{\theta}_0$ is used to initiate the algorithm.
2) Initiate $\mathbf{p}_0$ such that $\mathbf{p}_0 \sim N(0,\boldsymbol{M})$
3) Initiate the leapfrog algorithm with $(\boldsymbol{\theta},\mathbf{p})$ and run the algorithm for L time steps to obtain $(\boldsymbol{\theta}^*,\mathbf{p}^*)$.
4) Update the FEM to obtain the new analytic frequencies and then compute $H(\boldsymbol{\theta}^*,\mathbf{p}^*)$.
5) Accept $(\boldsymbol{\theta}^*,\mathbf{p}^*)$ with probability $\min(1,\ \exp\{-\beta_B \Delta H\})$.

Repeat steps (3–5) to for N_s samples.

In practice, the time step of the HMC method is bounded ($\delta t_{min} < \delta t < \delta t_{max}$). The performance of the HMC method degrades when the time step of the Störmer–Verlet integrated and/or the system size are large [26]. A significantly large time step increases the numerical errors caused by the integrator used to evaluate the Hamiltonian function. The error caused by the integrator can cause the Hamiltonian function to fluctuate and thus increase the rejection rate of the algorithm (no samples accepted in the case where $\delta t \geq \delta t_{max}$). To avoid a large rejection rate, the time step of this algorithm has to be less than δt_{max}. In the case where δt is too small, a high acceptance rate of HMC algorithm is obtained, however a large number of samples are needed to cover more space during the search (especially when $\delta t \leq \delta t_{min}$). On the other hand, relatively larger δt facilitates a significant jump from the existing samples and so a better exploration of the phase space. To overcome these inconveniences, an adjusted HMC algorithm based on the exploit of the Modified Hamiltonian function is proposed.

5. The Shadow Hybrid Monte Carlo method

The SHMC method is a generalization of HMC where the main idea of SHMC is to use a modified Hamiltonian approximation $\tilde{H}(\boldsymbol{\theta},\mathbf{p})$ to sample from the extended phase-space of the shadow Hamiltonian rather than the configuration space alone [26,29]. This approach overcomes the acceptance rate decrease of the HMC method when the system size N and/or time step δt is relatively large (The SHMC method expends the HMC time step). The formulation of the SHMC method requires the introduction of a parameter (a constant) c. Consider $\tilde{\rho}(\boldsymbol{\theta},\boldsymbol{p})$ as a target density function for SHMC where:

$$\tilde{\rho}(\boldsymbol{\theta},\mathbf{p}) \propto \exp(-\beta_B \tilde{H}(\boldsymbol{\theta},\mathbf{p})), \tag{16}$$

Please cite this article as: I. Boulkaibet, et al., Finite element model updating using the shadow hybrid Monte Carlo technique, Mech. Syst. Signal Process. (2014), http://dx.doi.org/10.1016/j.ymssp.2014.06.005

$$\tilde{H}(\boldsymbol{\theta},\mathbf{p}) = \max(H(\boldsymbol{\theta},\mathbf{p}),\ H_{[2k]}(\boldsymbol{\theta},\mathbf{p})-c). \tag{17}$$

where $H_{[2k]}(\boldsymbol{\theta},\mathbf{p})$ is an accurate shadow Hamiltonian defined in Section 6.The arbitrary constant c allows $H_{[2k]}(\boldsymbol{\theta},\mathbf{p})$ to depart from $H(\boldsymbol{\theta},\mathbf{p})$ since $H_{[2k]}(\boldsymbol{\theta},\mathbf{p})$ can have a significant separation from the original Hamiltonian $H(\boldsymbol{\theta},\mathbf{p})$. In SHMC, a new set of momentum $\boldsymbol{p}$ are generated from a Gaussian $(N(0,\boldsymbol{M})$ PDF. However, this momentum vector is accepted or rejected according to the Metropolis acceptance–rejection step (a non-separable Hamiltonian function). The complexity of drawing new momentums from the non-separable Hamiltonian function is solved by using the von Neumann approach [38,39]. This approach is summarized as follows: Consider a complicated target distribution $f(z)$ where samples must be generated from. The acceptance–rejection method generates a random number with a probability distribution function $f(z)$. First the probability distribution function is split as $f(z)=Cg(z)h(z)$ where $h(z)$ is a simple PDF, C is a constant and $0\le g(z)\le 1$. Then a random variable Z with PDF $h(z)$ is generated. Next a uniform random number U from (0,1) is generated. Finally, if $U\le g(z)$, then Z has the PDF $f(z)$. Otherwise repeat the process. In our case $f(z)=\tilde{\rho}(\boldsymbol{\theta},\mathbf{p})$ where:

$$\begin{aligned}\tilde{\rho}(\boldsymbol{\theta},\mathbf{p}) &= \exp(-\beta_B \max(H(\boldsymbol{\theta},\mathbf{p}),\ H_{[2k]}(\boldsymbol{\theta},\mathbf{p})-c))\\ &= \exp(-\beta_B H(\boldsymbol{\theta},\mathbf{p}))\min(1,\ \exp\{-\beta_B(H_{[2k]}(\boldsymbol{\theta},\mathbf{p})-c-H(\boldsymbol{\theta},\mathbf{p}))\})\end{aligned} \tag{18}$$

Then Eq.(18) can be written as:

$$\tilde{\rho}(\boldsymbol{\theta},\mathbf{p}) = \exp(-\beta_B V(\boldsymbol{\theta}))\exp(-\beta_B W(\boldsymbol{p}))\min(1,\ \exp\{-\beta_B(H_{[2k]}(\boldsymbol{\theta},\mathbf{p})-c-H(\boldsymbol{\theta},\mathbf{p}))\}) \tag{19}$$

Consider that $C=\exp(-\beta_B V(\boldsymbol{\theta}))$, $h(\boldsymbol{p})=\exp(-\beta_B W(\boldsymbol{p}))$ and $g(\boldsymbol{p})=\ \min(1,\ \exp\{-\beta_B(H_{[2k]}(\boldsymbol{\theta},\mathbf{p})-c-H(\boldsymbol{\theta},\mathbf{p}))\})$. In this case, the vector $\boldsymbol{p}$ is generated from the Gaussian distribution $h(\boldsymbol{p})$; then it is accepted or rejected according to $\min(1,\ \exp\{-\beta_B(H_{[2k]}(\boldsymbol{\theta},\mathbf{p})-c-H(\boldsymbol{\theta},\mathbf{p}))\})$.

The accepted–rejected step is repeated until a new momentum vector is accepted. Choosing the right parameter c can increase the efficiency of this method by reducing the number of attempts required to generate the new momentum vector.

Next, the system is integrated using an MD step. The SHMC algorithm can be summarized as follows [26,29]:

1. Set initial value $\boldsymbol{\theta}_0$.
2. Repeat for N_s samples.
   (a) **MC step:**
      a) Generate $\boldsymbol{p}$ such that $\boldsymbol{p}\sim N(0,\boldsymbol{M})$
      b) Accept with probability $(1,\ \exp\{-\beta_B(H_{[2k]}(\boldsymbol{\theta},\mathbf{p})-c-H(\boldsymbol{\theta},\mathbf{p}))\})$**,**
      c) Repeat until a new $\boldsymbol{p}$ is accepted
   (b) **MD step:**
      a) Initiate the extended leapfrog algorithm with $(\boldsymbol{\theta},\mathbf{p})$ and run the algorithm for L time steps to obtain $(\boldsymbol{\theta}^*,\mathbf{p}^*)$
      b) Update the FEM to obtain the new analytic frequencies and then compute $\tilde{H}(\boldsymbol{\theta}^*,\mathbf{p}^*)$
      c) Accept $(\boldsymbol{\theta}^*,\mathbf{p}^*)$ with probability $\min(1,\ \exp\{-\beta_B\Delta\tilde{H}\})$.

Both MC and MD steps are depending on the parameter c (see SHMC algorithm above) where this parameter has a significant effect on the simulation. When c is positively large, the SHMC algorithm matches the HMC algorithm (with different momentum) and this will decrease MD step acceptance rate (in the case that δt and/or system size are large), on the other hand the MC step acceptance rate increases. Conversely, a large negative c value increases the acceptance rate of the MD step and decreases the acceptance rate of the MC step (again in the case that δt and/or system size are large). In this paper, the value of c is chosen proportional to the average difference between the Hamiltonian and the shadow Hamiltonian. Finally, in order to calculate balanced values of the mean the results must be reweighted. This can be done by using $\rho(\boldsymbol{\theta},\mathbf{p})/\tilde{\rho}(\boldsymbol{\theta},\mathbf{p})$ before evaluating the averages. The average of an observable B is giving by [26,29]:

$$B=\frac{\sum_{i=1}^{Ns} B.a_i}{\sum_{i=1}^{Ns} a_i}, \text{where } a_i=\frac{\exp(-\beta_B H(\boldsymbol{\theta},\mathbf{p}))}{\exp(-\beta_B \tilde{H}(\boldsymbol{\theta},\mathbf{p}))} \tag{20}$$

6. Construction of the Shadow Hamiltonian

In Hamiltonian systems, the effects of discretization error could be analyzed by examining the "modified equations" of this system [27,28]. These equations are exactly satisfied by the (approximate) discrete solution [27,40,41]. The modified equations are defined by an asymptotic expansion in powers of the discretization parameter. The modified integrator is Hamiltonian if and only if the integrator is symplectic [26,27]. The integrator is symplectic if $\partial_y \boldsymbol{\varphi}(\boldsymbol{y})^T \boldsymbol{J} \partial_y \boldsymbol{\varphi}(\boldsymbol{y}) \equiv \boldsymbol{J}$, where $\boldsymbol{y}=\boldsymbol{\varphi}(\boldsymbol{y})$ is a numerical integrator, $\boldsymbol{J}=\begin{bmatrix} 0 & \boldsymbol{I} \\ -\boldsymbol{I} & 0 \end{bmatrix}$ and $\boldsymbol{I}$ is an identity matrix. There is also evidence that the numerical solution of symplectic integrators stays close to the solution of a modified Hamiltonian $H^{\delta t}(\boldsymbol{\theta},\boldsymbol{p})$ for very long times [26,27].

Please cite this article as: I. Boulkaibet, et al., Finite element model updating using the shadow hybrid Monte Carlo technique, Mech. Syst. Signal Process. (2014), http://dx.doi.org/10.1016/j.ymssp.2014.06.005

The Störmer–Verlet integrator is symplectic, which indicates that its modified differential equation is Hamiltonian. The modified Hamiltonian of this integrator is given by:

$$H^{\delta t} = H + \delta t^2\left(\frac{1}{12}\{W,\{W,V\}\} - \frac{1}{24}\{V,\{V,W\}\}\right) + \delta t^4\left(\frac{7}{5760}\{V,\{V,\{V,\{V,W\}\}\}\} - \frac{1}{720}\{W,\{W,\{W,\{W,V\}\}\}\}\right.$$
$$\left. + \frac{1}{360}\{V,\{W,\{W,\{W,V\}\}\}\} + \frac{1}{360}\{W,\{V,\{V,\{V,W\}\}\}\} - \frac{1}{480}\{V,\{V,\{W,\{W,V\}\}\}\} + \frac{1}{120}\{W,\{W,\{V,\{V,W\}\}\}\}\right) + \ldots \tag{21}$$

where the notation $\{A,B\} = \nabla_{\boldsymbol{\theta}} A \nabla_{\mathbf{p}} B - \nabla_{\mathbf{p}} A \nabla_{\boldsymbol{\theta}} B$ represents the Poisson bracket of two functions depending on $\boldsymbol{\theta}$ and $\mathbf{p}$. This formula is obtained from the symmetric Baker–Campbell–Hausdorff formula [42]. Skeel and Hardy [27] show how to compute a modified Hamiltonian using a splitting method. The goal is to compute:

$$H_{[2k]}(\boldsymbol{\theta},\mathbf{p}) = H^{\delta t}(\boldsymbol{\theta},\mathbf{p}) + \boldsymbol{O}(\delta t^{2k}) \tag{22}$$

where $H_{[2k]}(\boldsymbol{\theta},\mathbf{p})$ is a shadow Hamiltonian of order $2k$. The construction adds a new position variable and a conjugate momentum variable $\beta(t)$ to obtain an extended Hamiltonian $\overline{H}(\boldsymbol{y}) = (1/2)\boldsymbol{y}^T\boldsymbol{J}\boldsymbol{y}^T$ where $\boldsymbol{y} = [\boldsymbol{\theta}^T, \alpha, \mathbf{p}^T, \beta]^T$ and $\alpha = 1$. This extended Hamiltonian is homogeneous of order 2.The $\boldsymbol{y}$ is formed using a numerical solution of the extended Hamiltonian system and the final result satisfies Eq. (22). More details can be found in [26–29]. The formula for the 4th and 8th shadow Hamiltonians, $k=2$ and $k=4$, respectively are:

$$H_{[4]}(\boldsymbol{\theta},\mathbf{p}) = \boldsymbol{A}_{10} - \frac{1}{6}\boldsymbol{A}_{12} \tag{23}$$

$$H_{[8]}(\boldsymbol{\theta},\mathbf{p}) = \boldsymbol{A}_{10} - \frac{2}{7}\boldsymbol{A}_{12} - \frac{19}{210}\boldsymbol{A}_{14} + \frac{5}{42}\boldsymbol{A}_{30} + \frac{13}{105}\boldsymbol{A}_{32} - \frac{1}{140}\boldsymbol{A}_{34} \tag{24}$$

where the $\boldsymbol{A}_{ij}$ are defined as

$$\boldsymbol{A}_{ij} = \begin{cases} \mu\delta^i\theta\delta^j p - \delta^j\theta\mu\delta^i p - \mu\delta^i\beta & : j = 0 \\ \mu\delta^i\theta\delta^j p - \delta^j\theta\mu\delta^i p & : j \neq 0 \end{cases} \tag{25}$$

and $\delta\boldsymbol{\theta}$ represents the central difference of vector $\boldsymbol{\theta}$ defined by $\delta\boldsymbol{\theta} = \boldsymbol{\theta}^{(1/2)} - \boldsymbol{\theta}^{-(1/2)}$, and the averaging operator $\mu\boldsymbol{\theta}$ is similarly defined by $\mu\boldsymbol{\theta} = (1/2)(\boldsymbol{\theta}^{(1/2)} + \boldsymbol{\theta}^{-(1/2)})$. Note that $\boldsymbol{\theta}^{(1/2)} = \boldsymbol{\theta}(\boldsymbol{t} + (\boldsymbol{\delta}t/2))$ and $\boldsymbol{\theta}^{-(1/2)} = \boldsymbol{\theta}(\boldsymbol{t} - (\boldsymbol{\delta}t/2))$. To evaluate the leapfrog algorithm, we again use Eqs. (12)–(14), and we include the term $\beta(t)$, where $\beta(t)$ is evaluated according to

$$\beta(t+1) = \beta(t) + \delta t(\boldsymbol{\theta}(t)\nabla V(\boldsymbol{\theta}(t)) - 2V(\boldsymbol{\theta}(t)) \tag{26}$$

In this paper, the SHMC* (for convenience the * refers to both SHMC[4] and SHMC[8]) method is investigated on the updating of structural beam models. The first example is a simple unsymmetrical H-shaped aluminum structure and the second example is a GARTEUR SM-AG19 structure. The results of this method will be compared with those obtained by using an HMC method.

7. Unsymmetrical H-shaped structure

The unsymmetrical H-shaped aluminum structure is shown in Fig. 1. The structure was divided into 12 elements and each was modeled as an Euler–Bernoulli beam. The structure was excited at the position indicated by the double arrow and the acceleration was measured at 15 different positions. The structure was excited using an electromagnetic shaker and a roving accelerometer was used to measure the response. A set of 15 frequency-response functions were calculated. See [4] for more details about this structure.

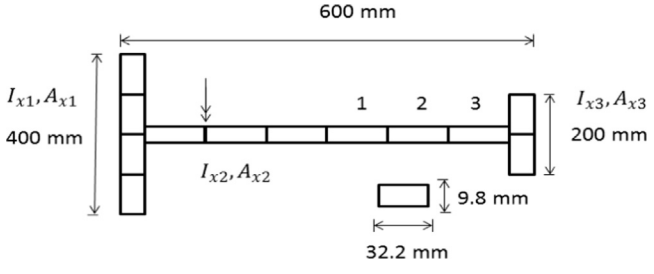

Fig. 1. The H-shaped aluminum structure.

Please cite this article as: I. Boulkaibet, et al., Finite element model updating using the shadow hybrid Monte Carlo technique, Mech. Syst. Signal Process. (2014), http://dx.doi.org/10.1016/j.ymssp.2014.06.005

7.1. H-beam simulation

The measured natural frequencies are: 53.9 Hz, 117.3 Hz, 2041.4 Hz, 254.0 Hz and 445.0 Hz. In this paper the moments of inertia and the cross section areas of the left, middle and right subsections of the beam (as labeled in Fig. 1) are updated. The updating parameter vector is thus $\boldsymbol{\theta} = \{I_{x1}, I_{x2}, I_{x3}, A_{x1}, A_{x2}, A_{x3}\}$. The Young's modulus for the beam is set to 7.2×10^{10} N/m^2 and the material density is set to 2785 kg/m^3. The temperature $T = 300$ K, $\beta_B = (1/K_B 300)$ where $K_B = 0.00198719$ kcal mol^{-1} K^{-1}. The updating parameters $\boldsymbol{\theta}$ are bounded by maximum values equal to $[3.73 \times 10^{-8}, 3.73 \times 10^{-8}, 3.73 \times 10^{-8}, 4.16 \times 10^{-4}, 4.16 \times 10^{-4}, 4.16 \times 10^{-4}]$ and minimum values are equal to $[1.7 \times 10^{-8}, 1.7 \times 10^{-8}, 1.7 \times 10^{-8}, 2 \times 10^{-4}, 2 \times 10^{-4}, 2 \times 10^{-4}]$. The boundaries help to keep the updated vector physically realistic.

In Eq. (6) the constant β_c of the posterior distribution is set equal 10. The coefficients α_i are set equal to $(1/\sigma_i^2)$, where σ_i^2 is the variance of the i th parameter and the variance vector is defined as $\sigma = [5 \times 10^{-8}, 5 \times 10^{-8}, 5 \times 10^{-8}, 5 \times 10^{-4}, 5 \times 10^{-4}, 5 \times 10^{-4}]$. The constant β_c and the variance σ in Eq. (6) are chosen so that the weight of

Table 1
Initial and updated parameters using HMC, SHMC^4 and SHMC^8.

	Initial $\boldsymbol{\theta}_0$	$\boldsymbol{\theta}$ vector, HMC method	$\frac{\sigma_i}{\mu_i}$ (%)=c.o.v.	$\boldsymbol{\theta}$ vector, SHMC^4 method	$\frac{\sigma_i}{\mu_i}$ (%) =c.o.v.	$\boldsymbol{\theta}$ vector, SHMC^8 method	$\frac{\sigma_i}{\mu_i}$ (%)=c.o.v.
I_{x1}	2.73×10^{-8}	2.21×10^{-8}	12.67	2.18×10^{-8}	12.60	2.24×10^{-8}	12.51
I_{x2}	2.73×10^{-8}	2.6×10^{-8}	1.37	2.49×10^{-8}	3.99	2.52×10^{-8}	1.47
I_{x3}	2.73×10^{-8}	2.9×10^{-8}	16.5	2.96×10^{-8}	14.93	2.94×10^{-8}	16.32
A_{x1}	3.16×10^{-4}	4.0×10^{-4}	1.39	4.05×10^{-4}	2.19	4.04×10^{-4}	1.54
A_{x2}	3.16×10^{-4}	2.3×10^{-4}	1.1	2.46×10^{-4}	2.10	2.41×10^{-4}	1.40
A_{x3}	3.16×10^{-4}	2.4×10^{-4}	1.95	2.25×10^{-4}	3.20	2.29×10^{-4}	1.78

Table 2
Natural frequencies and errors for HMC, SHMC^4 and SHMC^8.

Mode	Measured frequency (Hz)	Initial frequency (Hz)	Error (%)	Frequencies HMC method (Hz)	Error (%)	Frequencies SHMC^4 method (Hz)	Error (%)	Frequencies SHMC^8 method (Hz)	Error (%)
1	53.9	51.40	4.63	52.93 (0.17%)	1.8	52.94 (0.04%)	1.79	53.05 (0.05%)	1.58
2	117.3	116.61	0.59	118.82 (0.21%)	1.3	118.23 (0.15%)	0.79	118.7 (0.15%)	1.2
3	208.4	201.27	3.42	208.81 (0.24%)	0.2	207.91 (0.27%)	0.23	208.61 (0.27%)	0.1
4	254.0	247.42	2.59	254.41 (0.22%)	0.16	253.84 (0.17%)	0.06	253.91 (0.17%)	0.03
5	445	390.33	12.28	444.13 (0.41%)	0.2	443.0 (0.20%)	0.45	443.22 (0.20%)	0.40
Total average error	_	_	4.70	_	0.73	_	0.66	_	0.66

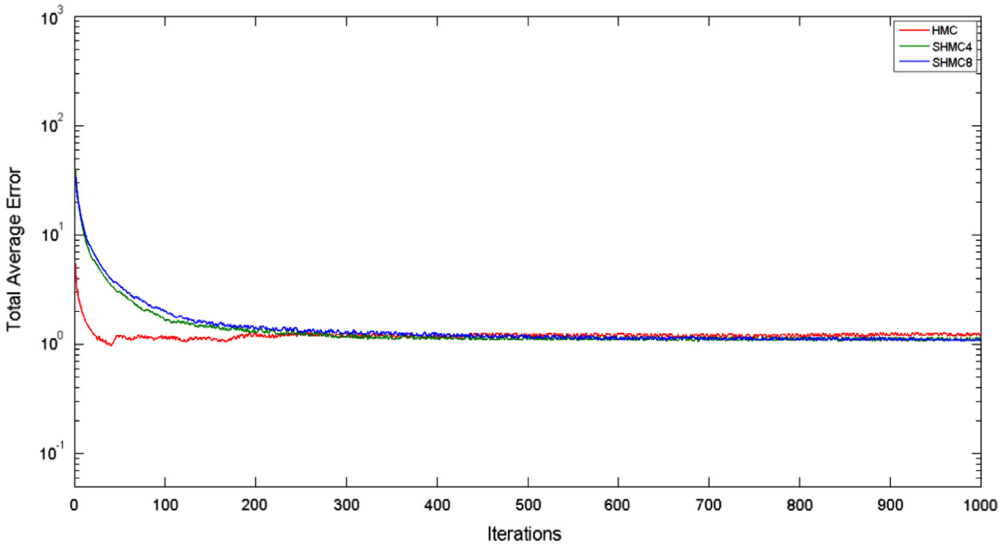

Fig. 2. The total average error for the algorithms.

Please cite this article as: I. Boulkaibet, et al., Finite element model updating using the shadow hybrid Monte Carlo technique, Mech. Syst. Signal Process. (2014), http://dx.doi.org/10.1016/j.ymssp.2014.06.005

the likelihood term in Eq. (6) will be greater than the second term in the PDF. The number of samples N_s is set to 1000, the time step is set to 0.0045 s and the constant $c=0.001$. Each algorithm has been implemented over 20 independent runs. The final results tabulated in Tables 1 and 2 are the average of these 20 runs (different initial momentum in each run gives slightly different results).

Table 1 presents the initial, updated and corresponding coefficient of variation values of the updating vector obtained by each method. The coefficient of variation (c.o.v.) represents the estimated standard deviation divided by the estimated mean $\boldsymbol{\theta}$ for each algorithm. The estimations of the middle beam parameters are better than the left and the right beams parameters, and this can be seen from the values of the coefficient of variation in Table 1 (the standard deviation of the middle beam updated parameters are lower than those obtained for both left and right beams). The reason could be that the structure was excited at the position indicated by the double arrow (located on the middle beam), which means more information of the middle beam is used for the updating process.

Table 2 presents the updated natural frequencies for each mode (the coefficient of variation inside the parenthesis represents the estimated standard deviation divided by the estimated frequency), the absolute mode error and the final model error in percentage form for all three algorithms. The percentage error is defined by the differences between the updated value of the natural frequency and its experimental value divided by the experimental value. Different methods have been used to update the H-shaped beam structure [4] where the total average error obtained by using Nelder Mead (NM) Simplex method is 2.14% while the Genetic Algorithm (GA) reduced this error to 1.1%. The Response-Surface (RS) method produced a total average error equal to 1.84% while the Particle Swarm Optimization (PSO) algorithm reduced the error to 0.4%.

The error between the first measured natural frequency and that of the initial model was 4.63%. When applying HMC method this error was reduced to 1.8% and by implementing SHMC^{4,8} it was reduced to 1.79% and 1.58%, respectively. In overall, the updated FEM natural frequencies for all three algorithms are better than the initial FEM. The SHMC algorithms produced slightly better total error results than the HMC algorithm. The updating using these methods improved the error from 4.7% to 0.66% which is an acceptable percentage comparing to the results previously obtained by NM, GA and RS methods.

Fig. 2 shows the total average error vs. number of iterations for the three algorithms for 1000 iterations. The y-axis (Total Average Error) is plotted by using the base 10 logarithmic scale. Fig. 2 is obtained by evaluating the mean value of the samples at each iteration (i) for all algorithms. The total average error is computed from the average of the errors between the analytical and the experimental frequencies. The results obtained shows that the three algorithms converge fast and within the first 200 iterations (200 samples will be enough to obtain good updated parameters). The constant $c=0.001$ resulted in a reduced average error (see Table 2). The choice of a poor c may degrade the performance of the MC step because the rejection rate of the MC step decreases when $c$is small. This can be very expensive in terms of momentum sampling time.

The efficiency of HMC and SHMC algorithms directly depends on the chosen time step δt. A large time step helps to sample from an extended phase-space (cover more space) during the search operation. This can cause faster convergence but with few samples. The time step of $\delta t = 0.0045$ s provided a good sampling acceptance rate for all methods: HMC and SHMC^{4,8} (99.9%). When times step δt increases, the SHMC* method samples with reasonable efficiency and keeps the acceptance rate higher than the HMC method (see Fig. 3). The SHMC algorithm can be viewed as a generalization of HMC algorithm that samples from a PDF in all of phase space. However, these methods show some performance degradations as δt approaches its upper bound due to the instabilities in the MD integrator and the faster motions of the system [26].

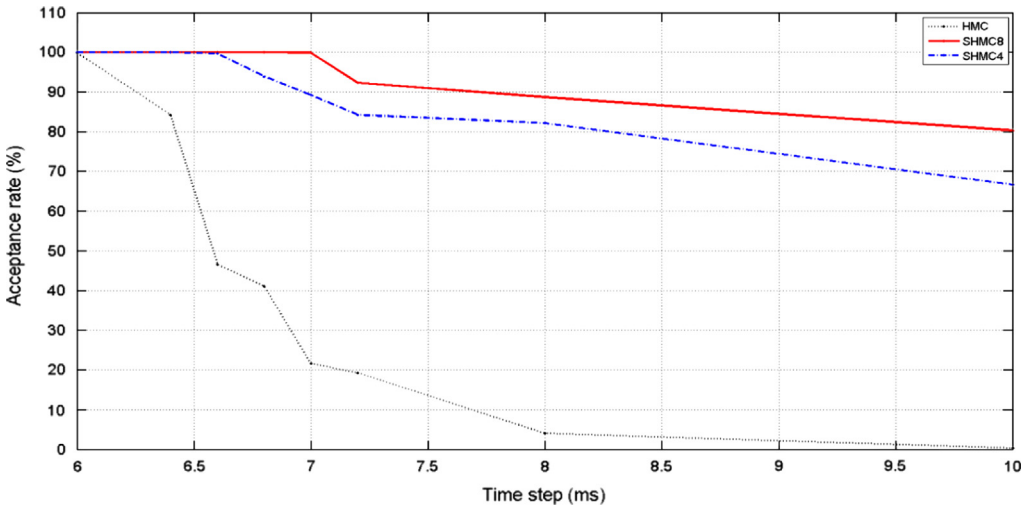

Fig. 3. Sampling acceptance rate at different time steps for the algorithms.

Please cite this article as: I. Boulkaibet, et al., Finite element model updating using the shadow hybrid Monte Carlo technique, Mech. Syst. Signal Process. (2014), http://dx.doi.org/10.1016/j.ymssp.2014.06.005

To verify this, different time step are used to run all three algorithms and obtain the acceptance rate vs. time step graph. The acceptance rate (AR) of both algorithms is evaluated by calculating the ratio of accepted moves to total moves attempted. Fig. 3 shows the sampling acceptance rate for time steps between 0.006 s and 0.01 s.

The HMC acceptance rate starts decreasing from the time step of 0.006 s (99.7%) until it reaches 0% (no updated values for the $\boldsymbol{\theta}$ vector) at time step 0.01 s (the upper bound time step of the HMC algorithm is $\delta t_{max} = 0.01$ s). On the other hand, the SHMC methods maintain a good acceptance rate. At time step 0.006 s both SHMC[4,8] have an acceptance rate equal to 99.9%. The SHMC[4] maintains this value until $\delta t = 0.0066$ s and starts decreasing from $\delta t = 0.0068$ s (93.9%) to reach an acceptance rate equal to 66% at time step $\delta t = 0.01$ s which is better than the HMC algorithm (upper bound time step of the SHMC[4] algorithm is larger than 0.01 s.). The SHMC[8] maintains the initial acceptance rate for larger time steps (until $\delta t = 0.007s$) but then gradually reduces to 80.3% by the $\delta t = 0.01$ s time step. A large time step marginally affects all three algorithms' results where the acceptance rate of SHMC[8] algorithm decreases to 80.3% for $\delta t = 0.01$ s which is far better than the HMC algorithm. In this example, the SHMC method successfully extended the time step upper bound where $\delta t_{max}^{SHMC} \geqslant 0.01$ s. The value of the constant c used to plot Fig. 3 is equal to 0.001.

The results from Table 2 are not conclusive on which algorithm is better for this relatively simple FEM problem. To explore this issue further a more complex structure is considered in the next section.

8. The Garteur Sm-Ag19 structure

The GARTEUR SM-AG19 structure was used as a benchmark study by 12 members of the GARTEUR Structures and Materials Action Group 19 [43–48]. The aeroplane has a length of 1.5 m and a width of 3 m. The depth of the fuselage is 15 cm with a thickness of 5 cm. The material used was aluminum and the overall mass is 44 kg. In order to increase the damping, a $1.1 \times 76.2 \times 1700$ mm^3 viscoelastic constraining layer was bonded to the wings. Further details are described in reference [44]. Fig. 4 shows the finite element model (beam) of the aeroplane. In our models all element materials are considered to be standard isotropic. The beam elements of the model were modeled as Euler–Bernoulli elements

8.1. Garteur simulation

The experimental test data used in this work is data obtained by DLR Göttingen, Germany in above study. The measured natural frequencies (Hz) data are: 6.38, 16.10, 33.13, 33.53, 35.65, 48.38, 49.43, 55.08, 63.04, 66.52 Hz. The parameters of the structure to be updated are the right wing moments of inertia and torsional stiffness ($R\_I_{min}, R\_I_{max}, R\_I_{tors}$), the left wing moments of inertia and torsional stiffness ($L\_I_{min}, L\_I_{max}, L\_I_{tors}$), the vertical tail moment of inertia (VTP_I_{min}) and the overall structure's density ρ. The temperature $T = 300$ K, $\beta_B = (1/K_B 300)$ where $K_B = 0.00198719$ kcal mol^{-1} K^{-1}. The update vector is thus given by $\boldsymbol{\theta} = [\rho, VTP\_I_{min}, L\_I_{min}, L\_I_{max}, R\_I_{min}, R\_I_{max}, L\_I_{tors}, R\_I_{tors}]$. The Young's modulus for the aeroplane is also set to 7.2×10^{10} N/m^2. In Eq. (6) the constant β_c of the posterior distribution is set equal 100. All coefficients α_i are set equal to $(1/\sigma_i^2)$, where σ_i^2 is the variance of the ith parameter and $\sigma = [5 \times 10^2, 5 \times 10^{-9}, 5 \times 10^{-9}, 5 \times 10^{-7}, 5 \times 10^{-9}, 5 \times 10^{-7}, 5 \times 10^{-8}, 5 \times 10^{-8}]$. The mean values of the updated vector and their bounds are given in Tables 3 and 4 respectively. The time step is set at $\delta t = 3$ ms and the number of samples is $N_s = 1000$. The constant of

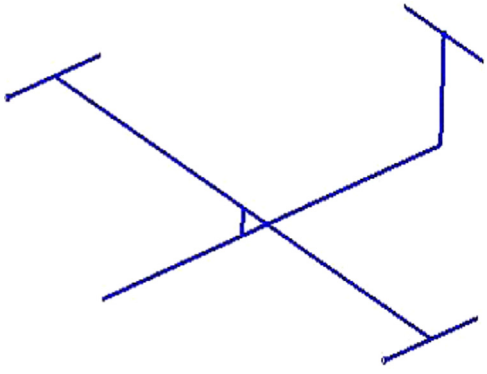

Fig. 4. FEM Garteur Structure.

Table 3
The initial values of the updating parameters for the GARTEUR example.

Parameter	ρ (kg/m^3)	VTP_I_{min} (10^{-9} m^4)	L_I_{min} (10^{-9} m^4)	L_I_{max} (10^{-7} m^4)
	2785	8.34	8.34	8.34
Parameter	L_I_{tors} (10^{-8} m^4)	R_I_{min} (10^{-9} m^4)	R_I_{max} (10^{-7}m^4)	R_I_{tors} (10^{-8}m^4)
	4.0	8.34	8.34	4.0

Please cite this article as: I. Boulkaibet, et al., Finite element model updating using the shadow hybrid Monte Carlo technique, Mech. Syst. Signal Process. (2014), http://dx.doi.org/10.1016/j.ymssp.2014.06.005

Table 4
The bounds of the updating parameters for the GARTEUR example.

ρ	*Max* 3500	*Min* 2500
VTP_I_{min}	12×10^{-9}	5×10^{-9}
L_I_{min}	12×10^{-9}	5×10^{-9}
L_I_{max}	12×10^{-7}	5×10^{-7}
R_I_{min}	12×10^{-9}	5×10^{-9}
R_I_{max}	12×10^{-7}	5×10^{-7}
L_I_{tors}	6×10^{-8}	3×10^{-8}
R_I_{tors}	6×10^{-8}	3×10^{-8}

Table 5
Initial and updated parameter values for the 3ms time step.

	Initial (the mean vector) $\boldsymbol{\theta}_0$	HMC Method $\delta t=3$ ms $\boldsymbol{\theta}$	$\frac{\sigma_i}{\mu_i}$(%) c.o.v	SHMC^4 Method $\delta t=3$ ms $\boldsymbol{\theta}$	$\frac{\sigma_i}{\mu_i}$(%) c.o.v	SHMC^8 Method $\delta t=3$ ms $\boldsymbol{\theta}$	$\frac{\sigma_i}{\mu_i}$(%) c.o.v
ρ	2785	2667.33	1.97	2666.85	2.27	2686.97	2.98
VTP_I_{min}	8.34×10^{-9}	6.938×10^{-9}	5.62	6.961×10^{-9}	5.50	7.154×10^{-9}	6.92
L_I_{min}	8.34×10^{-9}	10.12×10^{-9}	2.34	10.12×10^{-9}	2.27	10.13×10^{-9}	3.38
L_I_{max}	8.34×10^{-7}	7.899×10^{-7}	2.61	7.919×10^{-7}	2.75	8.018×10^{-7}	3.34
R_I_{min}	8.34×10^{-9}	10.15×10^{-9}	2.13	10.13×10^{-9}	2.21	10.12×10^{-9}	3.38
R_I_{max}	8.34×10^{-7}	6.11×10^{-7}	3.14	6.096×10^{-7}	4.02	6.109×10^{-7}	4.21
L_I_{tors}	4×10^{-8}	4.043×10^{-8}	1.95	4.036×10^{-8}	2.09	4.024×10^{-8}	2.61
R_I_{tors}	4×10^{-8}	3.571×10^{-8}	2.17s	3.563×10^{-8}	2.49	3.573×10^{-8}	3.18

Table 6
Modal results and Errors for all algorithms at two different time steps.

Mode	Measured frequency (Hz)	Initial FEM frequencies (Hz)	Error (%)	HMC frequencies (Hz) $\delta t=3$ ms	Error (%)	SHMC^4 frequencies (Hz) $\delta t=3$ ms	Error (%)	SHMC^8 frequencies (Hz) $\delta t=3$ ms	Error (%)
1	6.38	5.71	10.47	6.313 (0.95%)	1.06	6.312 (1.30%)	1.07	6.301 (1.83%)	1.23
2	16.10	15.29	5.01	15.866 (0.81%)	1.45	15.875 (1.38%)	1.40	15.93 (1.94%)	0.98
3	33.13	32.53	1.82	32.236 (0.75%)	2.70	32.238 (1.43%)	2.69	32.33 (2%)	2.42
4	33.53	34.95	4.23	33.90 (0.76%)	1.10	33.88 (1.52%)	1.04	33.93 (2.13%)	1.19
5	35.65	35.65	0.012	35.643 (0.31%)	0.02	35.62 (1.45%)	0.083	35.589 (2.04%)	0.17
6	48.38	45.14	6.69	48.84 (0.61%)	0.95	48.80 (1.36%)	0.87	48.783 (1.90%)	0.83
7	49.43	54.69	10.65	49.871 (1.45%)	0.89	49.86 (1.61%)	0.88	49.702 (2.26%)	0.55
8	55.08	55.60	0.94	54.364 (0.83%)	1.30	54.418 (1.47%)	1.20	54.591 (2.06%)	0.89
9	63.04	60.15	4.59	63.888 (0.68%)	1.35	63.896 (1.39%)	1.36	63.828 (1.95%)	1.25
10	66.52	67.56	1.57	67.446 (0.029%)	1.39	67.447 (1.48%)	1.39	67.449 (2.07%)	1.40
Total Average errors	_	_	4.6	_	1.22	_	1.20	_	1.09

$c=0.01$ was found to provide good results. Each algorithm has been run over 10 independent simulations. The final results tabulated in Tables 5 and 6 are the average of these 10 runs.

A number of studies have been made to update the GARTEUR SM-AG19 structure. Mares et al. [49] reduced the error to 0.66% by applying a sensitivity method to update a number of parameters. Link et al. [50] summarized the results obtained by seven participants where each participant updated different set of parameters using different computational methods. The average error varied between 0.69% and 2.03% for all participant results. A modification was made to the wing of the original structure and this time the average error between the participants varied being between 1.02% and 1.50%. In this study two MCMC algorithms are implemented to update the FEM of the above structure.

Table 5 presents the initial value (the mean material or geometric value) of the update vector $\boldsymbol{\theta}$ and the updated values obtained by HMC and the SHMC^{4,8} methods for the time step of $\delta t = 0.003$ s. The corresponding coefficient of variation (c.o.v) is also presented.

The updated parameters obtained by all of the algorithms are physically realistic. There is a small difference between the final updated values obtained by the HMC and both SHMC algorithms. This is because of the way that the SHMC algorithms use the non-separable Shadow Hamiltonian function for sampling. Furthermore the SHMC algorithms use two extra parameters when evaluating the MC and MD step (the constants c and $\beta(t)$).

Please cite this article as: I. Boulkaibet, et al., Finite element model updating using the shadow hybrid Monte Carlo technique, Mech. Syst. Signal Process. (2014), http://dx.doi.org/10.1016/j.ymssp.2014.06.005

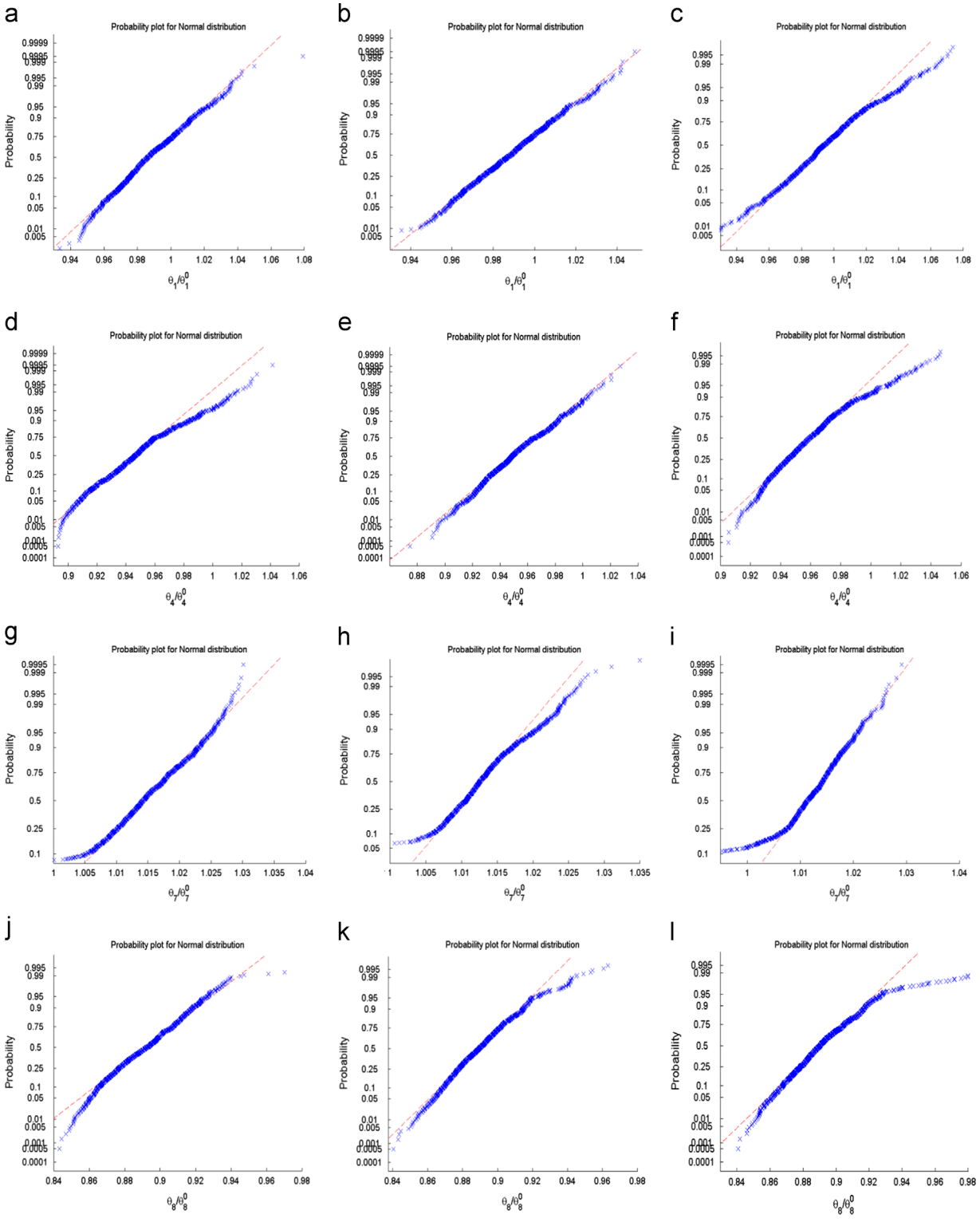

Fig. 5. Normal probability plots for $\rho(\theta_1)$, $L\_I_{max}(\theta_4)$, $L\_I_{tors}(\theta_7)$ and $R\_I_{tors}(\theta_8)$ from HMC, SHMC^4 and SHMC^8 algorithms for the GARTEUR example. Straight line indicates a Gaussian distribution of data. The normalization constants θ_1^0 θ_4^0, θ_7^0 and θ_8^0 are the initial values for, for, L_I_{max}, L_I_{tors} and R_I_{tors} for each simulation (see Table 3). a) Normal probability plot for ρ (HMC), b) Normal probability plot for ρ (SHMC^4), c) Normal probability plot for ρ (SHMC^8), d) Normal probability plot for L_I_{max} (HMC), e) Normal probability plot for L_I_{max} (SHMC^4), f) Normal probability plot for L_I_{max} (SHMC^8), g) Normal probability plot for L_I_{tors} (HMC), h) Normal probability plot for L_I_{tors} (SHMC^4), i) Normal probability plot for L_I_{tors} (SHMC^8), j) Normal probability plot for L_I_{tors}(HMC), k) Normal probability plot for R_I_{tors} (SHMC^4) and l) Normal probability plot for R_I_{tors} (SHMC^8).

Please cite this article as: I. Boulkaibet, et al., Finite element model updating using the shadow hybrid Monte Carlo technique, Mech. Syst. Signal Process. (2014), http://dx.doi.org/10.1016/j.ymssp.2014.06.005

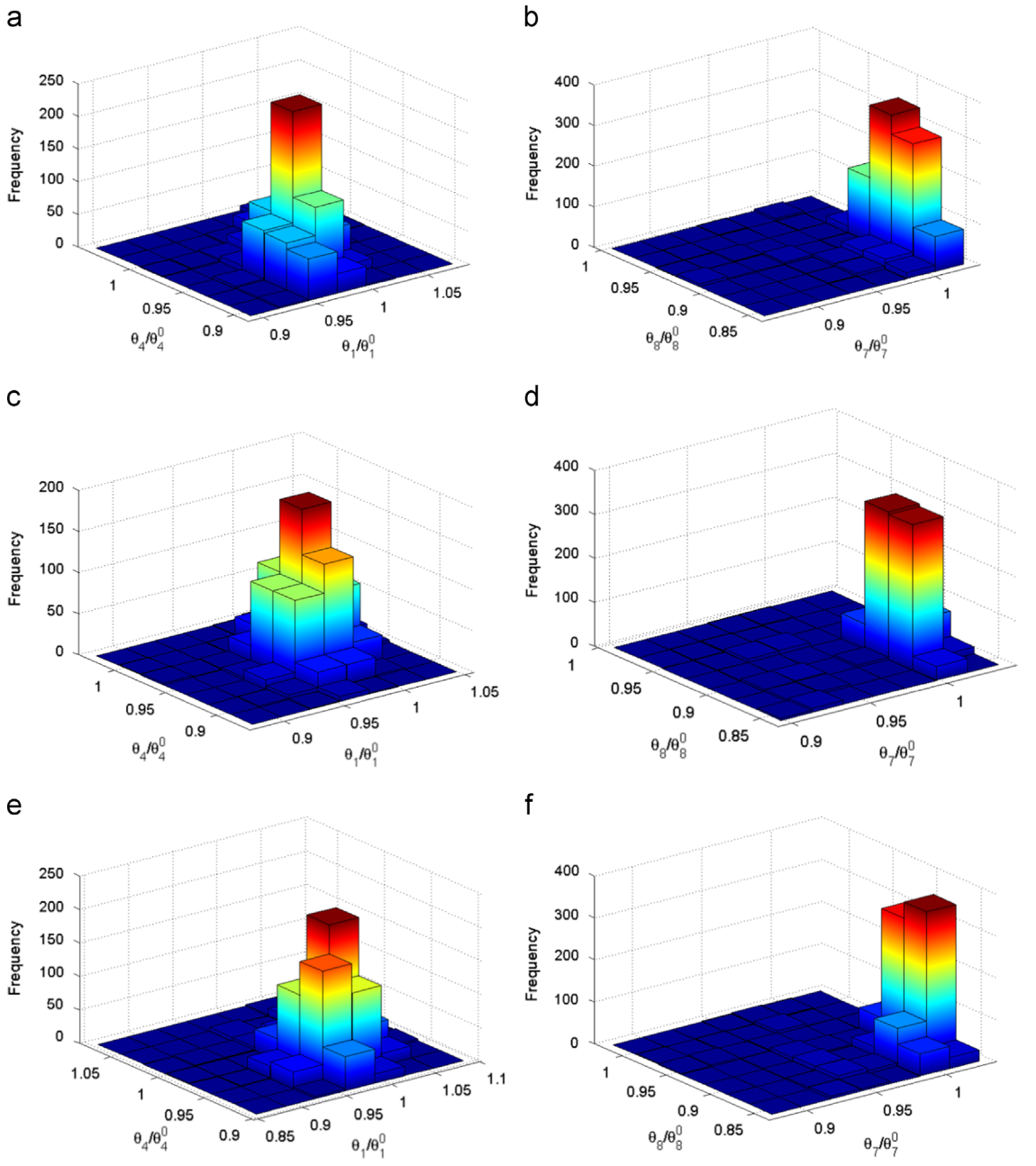

Fig. 6. 2-Dimensional histogram plots for ρ *vs* *L_I*$_{max}$ and *R_I*$_{tors}$ *vs* *R_I*$_{tors}$ for HMC and SHMC[4,8] algorithms for the GARTEUR example. The red area in the graphs indicates the high probability area. a) 2-Dimensional histogram plot for (ρ *vs* *L_I*$_{max}$) (HMC), b) 2-Dimensional histogram plot for (*L_I*$_{tors}$ *vs* *R_I*$_{TORS}$) (HMC), c) 2-Dimensional histogram plot for (*L_I*$_{max}$) (SHMC[4]), d) 2-Dimensional histogram plot for (*L_I*$_{TORS}$ *vs* *R_I*$_{tors}$) (SHMC[4]), e) 2-Dimensional histogram plot for (ρ *vs* *L_I*$_{max}$) (SHMC[8]) and f) 2-Dimensional histogram plot for (*L_I*$_{tors}$ *vs* *R_I*$_{tors}$) (SHMC[8]).

It can be seen that the coefficient of variation is small for all algorithms (less than 6% for both HMC and SHMC[4], and less than 7% for the SHMC[8] algorithm). The time step used provides a good acceptance sampling rate of 99.9% for all algorithms. The additional parameter, c, of SHMC algorithm is used to control the difference between the modified and the true Hamiltonian function. In this paper, the value of *c* is chosen so that the modified Hamiltonian function can depart from the true Hamiltonian function. However, different choices of *c* might obtain better errors.

Fig. 5 presents the Gaussian probability plots for four of the eight updated parameters using the three algorithms. This plot is a good way to verify whether the updating parameters follow a Gaussian distribution (which is difficult to decide from histogram plots). In these figures θ_i refers to the sequential numbering of the updating parameters in the updating vector, i.e. $\theta_i=\rho$ (density) and θ_4 refers to *L_I*$_{max}$ as listed on Table 4. The effect of the non-separable Shadow Hamiltonian

Please cite this article as: I. Boulkaibet, et al., Finite element model updating using the shadow hybrid Monte Carlo technique, Mech. Syst. Signal Process. (2014), http://dx.doi.org/10.1016/j.ymssp.2014.06.005

function and the SHMC reweighting step are more pronounced in the graphs shown in Fig. 5 where all algorithms give different probability distribution form. The density distribution from both HMC and SHMC[4] methods is almost ideal Gaussian distributed (display some non-Gaussian behavior in the tails). The same comment can be made for L_I_{max}

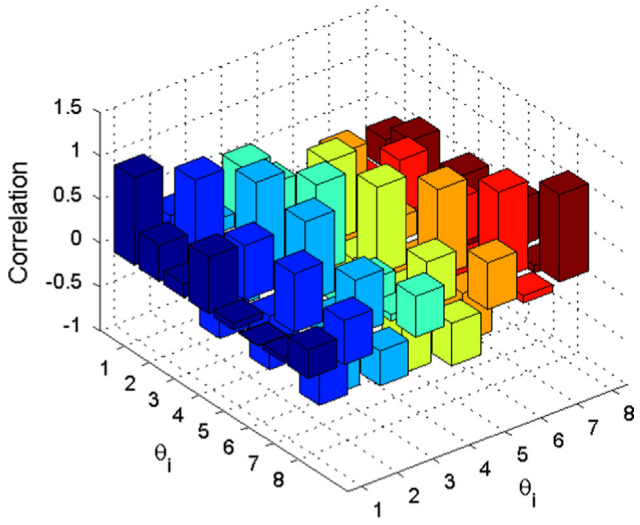

Fig. 7. The correlation between the updated parameters (HMC algorithm).

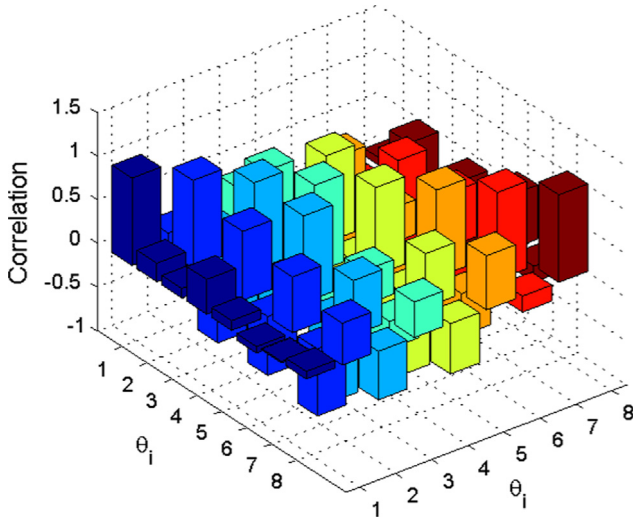

Fig. 8. The correlation between parameters (SHMC[8] algorithm).

Table 7
Initial and updated parameter values for the 4.8ms time step.

	Initial (the mean vector) $\boldsymbol{\theta}_0$	HMC method $\delta t = 4.8$ ms $\boldsymbol{\theta}$	SHMC[4] method $\delta t = 4.8$ ms $\boldsymbol{\theta}$	$\frac{\sigma_i}{\mu_i}$ (%) c.o.v	SHMC[8] method $\delta t = 4.8$ ms $\boldsymbol{\theta}$	$\frac{\sigma_i}{\mu_i}$ (%) (c.o.v)
L_I_{min}	2785	2785	2737.66	3.42	2727.91	2.52
VTP_I_{min}	8.34×10^{-9}	8.34×10^{-9}	7.467×10^{-9}	10.54	7.456×10^{-9}	5.45
L_I_{min}	8.34×10^{-9}	8.34×10^{-9}	10.15×10^{-9}	1.63	10.16×10^{-9}	0.97
L_I_{max}	8.34×10^{-7}	8.34×10^{-7}	8.184×10^{-7}	2.93	8.204×10^{-7}	2.90
R_I_{min}	8.34×10^{-9}	8.34×10^{-9}	10.14×10^{-9}	1.52	10.14×10^{-9}	1.19
R_I_{max}	8.34×10^{-7}	8.34×10^{-7}	6.305×10^{-7}	2.30	6.079×10^{-7}	1.45
L_I_{tors}	4×10^{-8}	4×10^{-8}	3.969×10^{-8}	3.24	4.006×10^{-8}	2.08
R_I_{tors}	4×10^{-8}	4×10^{-8}	3.623×10^{-8}	1.81	3.586×10^{-8}	1.48

Please cite this article as: I. Boulkaibet, et al., Finite element model updating using the shadow hybrid Monte Carlo technique, Mech. Syst. Signal Process. (2014), http://dx.doi.org/10.1016/j.ymssp.2014.06.005

distribution obtained by SHMC[4] algorithm. The HMC algorithm produces distributions close to the Gaussian one for both L_I_{tors} and R_I_{tors}. In general, distributions obtained by the three algorithms showed non-Gaussian behavior.

Fig. 6 represents the 2-Dimensional histogram plots for the pairs, $\rho(\theta_1)$*vs* $L\_I_{max}(\theta_4)$ and $L\_I_{tors}(\theta_7)$ *vs* $R\_I_{tors}(\theta_8)$. The plots shows the region of most probable values of the updated parameters where both HMC and SHMC[4,8] algorithms were able to find parameters with high probability (the red region in Fig. 6). Also, all algorithms HMC and SHMC[4,8] produces different histograms (different samples). This can be attributed to the SHMC reweighting step and also the degree of the shadow Hamiltonian function.

Figs. 7 and 8 show the correlation between all updated parameters for both algorithms, namely HMC and SHMC[8] (SHMC[4] and SHMC[8] had almost the same correlations). Small values indicate that both parameters are weakly correlated (<0.3), however large values (>0.7) indicate that the parameters are highly correlated while zero indicates that the parameters are not correlated. A positive correlation indicates that the variables are positively related while a negative correlation indicates the opposite. In the current study Figs. 7 and 8 indicate that for both algorithms, all parameters are correlated (all values are not 0). Both algorithms indicate that the pairs (R_I_{min}, R_I_{max}), (L_I_{min}, R_I_{max}) and (R_I_{max}, L_I_{min}) are highly correlated while (ρ, R_I_{max}), (ρ, R_I_{max}) and (ρ, R_I_{min}) are weakly correlated.

Table 6 shows the modal results and output errors for the different sampling algorithms. The values inside the parenthesis represent the coefficient of variation (c.o.v). The results show that the updated FEM natural frequencies are better than the initial FEM for all algorithms. The error between the second measured natural frequency and that of the initial model is 5.01%. With the HMC method this error is reduced to 1.45% and by implementing the SHMC[4] and SHMC[8] it was further reduced to 1.40% and 0.98% respectively. A similar observation can be made for the fourth, sixth, seventh, eighth and ninth natural frequencies. The SHMC* (both SHMC[4] and SHMC[8]) produce a smaller final total average error compared to

Table 8
Modal results and errors for all algorithms for a time step of 4.8 ms.

Mode	Measured frequency (Hz)	Initial FEM frequencies (Hz)	Error (%)	Frequencies HMC method (Hz) $\delta t=4.8$ ms	Error (%)	Frequencies SHMC[4] method (Hz) $\delta t=4.8$ ms	Error (%)	Frequencies SHMC[8] method (Hz) $\delta t=4.8$ ms	Error (%)
1	6.38	5.71	10.47	5.71	10.47	6.284 (2.06%)	1.50	6.291 (2.15%)	1.40
2	16.10	15.29	5.01	15.29	5.01	16.043 (2.19%)	0.35	16.049 (2.28%)	0.32
3	33.13	32.53	1.82	32.53	1.82	32.453 (2.26%)	2.04	32.454 (2.36%)	2.04
4	33.53	34.95	4.23	34.95	4.23	33.991 (2.4%)	1.38	33.993 (2.50%)	1.38
5	35.65	35.65	0.012	35.65	0.012	35.517 (2.30%)	0.37	35.545 (2.40%)	0.29
6	48.38	45.14	6.69	45.14	6.69	48.879 (2.15%)	1.03	48.559 (2.24%)	0.37
7	49.43	54.69	10.65	54.69	10.65	49.367 (2.55%)	0.13	49.451 (2.65%)	0.043
8	55.08	55.60	0.94	55.60	0.94	55.093 (2.32 %)	0.02	54.888 (2.42%)	0.35
9	63.04	60.15	4.59	60.15	4.59	63.628 (2.19%)	0.93	63.717 (2.29%)	1.07
10	66.52	67.56	1.57	67.56	1.57	67.458 (2.34%)	1.41	67.450 (2.44%)	1.40
Total Average errors	_	_	4.6	_	4.6	_	0.92	_	0.87

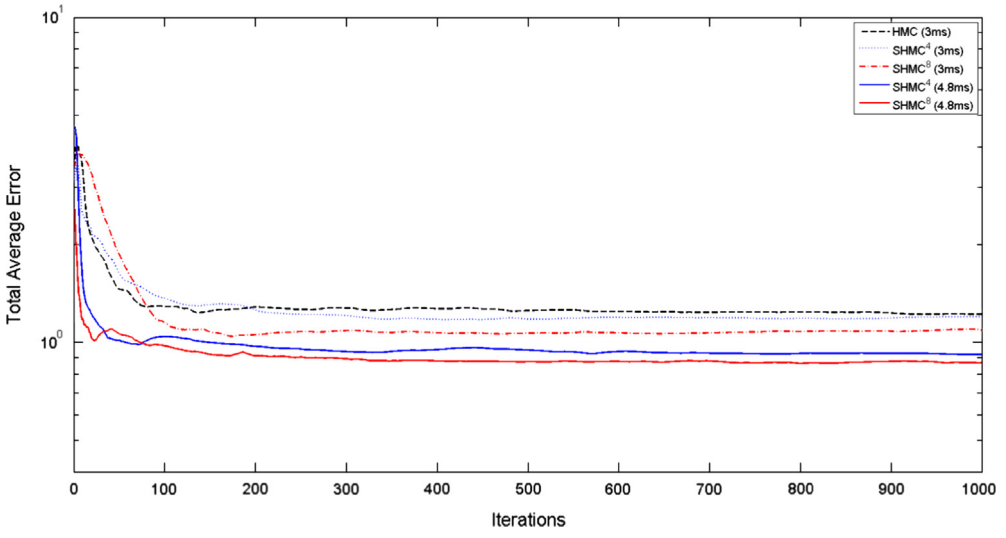

Fig. 9. The total average error for the three algorithms for different time steps.

Please cite this article as: I. Boulkaibet, et al., Finite element model updating using the shadow hybrid Monte Carlo technique, Mech. Syst. Signal Process. (2014), http://dx.doi.org/10.1016/j.ymssp.2014.06.005

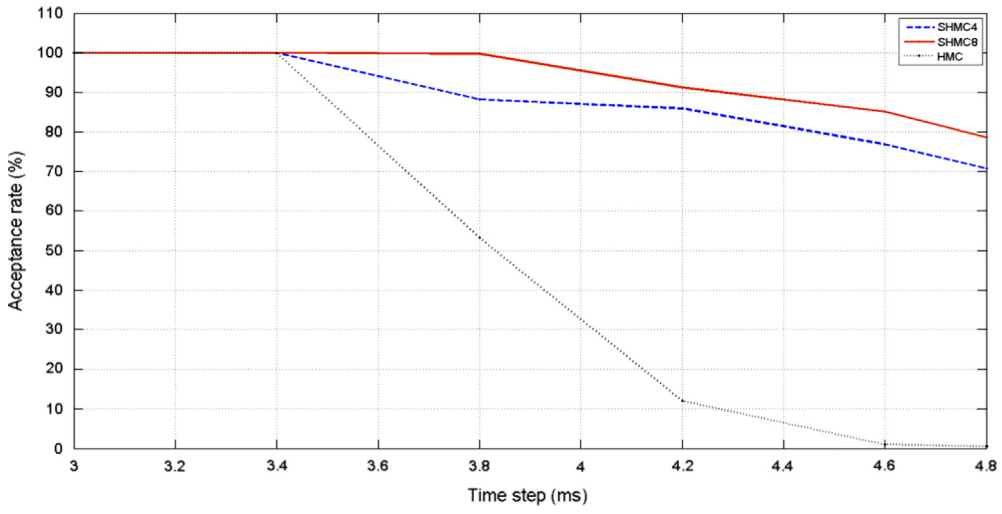

Fig. 10. The acceptance rate obtained for different time steps for all algorithms.

that obtained by the HMC algorithm for the same initial time step. The initial total average error was 4.6% but after using the HMC, SHMC^4 and SHMC^8 methods it reduce to 1.22%, 1.20% and 1.09% respectively. Another observation can be made from the results of Table 8 which indicate that all algorithms give a robust estimation of the updated parameters which can be verified by the low (less than 3%) values of c.o.v for all modes.

The time step, $\delta t = 0.003$ s, provides a good acceptance sampling rate for all methods: HMC and SHMC (99.9%). Fig. 9 shows the total average error versus number of iterations for the three algorithms. Convergence results for two time steps $\delta t = 0.003$ s and $\delta t = 0.0048$ s are plotted on the same graph. In these simulations $c = 0.01$. The y-axis (Total Average Error) is plotted by using the base 10 logarithmic scale. Fig. 9 shows the efficiency of these algorithms where 150–200 iterations (150–200 samples) will be enough to obtain a good average error. The three algorithm almost have the same convergence rate when time step $\delta t = 0.003$ s. However, the error decreases faster for both SHMC^{4,8} algorithms when the time step is $\delta t = 0.0048$ s (convert in the first 100 iterations). This indicates that the SHMC* algorithm is more efficient that the HMC algorithm for large time steps.

The updated parameter results of the $\delta t = 0.0048$ s time step and their coefficient of variation (c.o.v) are given in Table 7. The time step is large enough to allow significant jumps of the algorithm during the searching process. This leads to better modeling results, see Table 8. In this setting the HMC method gives poor updating parameters where no updating happened (the same initial values). This is because the time step $\delta t = 0.0048s$ does not conserve the Hamiltonian function which leads to a high rejection rate in the algorithm. The use of this time step caused significant numerical errors of the integrator used to evaluate the pair $(\boldsymbol{\theta}, \mathbf{p})$. In this case, the Hamiltonian function starts fluctuating with time which causes a sudden decrease of the acceptance rate (the acceptance rate decreases to less than 1% when the time step is $\delta t = 0.0048$ s). The acceptance rate for SHMC^4 is 71% and 78% for the SHMC^8 algorithm, which is an acceptable rate compared to that for the HMC method. The estimation error (c.o.v) is small for SHMC* algorithms where the error is less than 11% for SHMC^4 algorithm and less than 6% for the SHMC^8 algorithm.

Changing the time step for both methods provided different results from those in Table 5. In the case where the time step is increased ($\delta t = 0.0048$ s), the SHMC method improves the most. This can be seen in Table 8 where the total average error is reduced to 0.92% for SHMC^4 algorithm and 0.87% for SHMC^4 algorithm. However, this is not the case for HMC where the acceptance rate decreases to less than 1% and the updated vector obtained from the HMC does not improve the FEM results. Fig. 10 shows the acceptance rate versus time step. The acceptance rate for both methods is 99.9% when the time step is 3 ms. The acceptance rate starts decreasing when the time step increases for both methods but this decrease is faster and more significant in the case of the HMC method. When the time step $\delta t = 3.4$ ms, the acceptance rate for the HMC method decreases slightly to 98.7% and stays the same for the SHMC* methods (99.9% for both). When the time step is 3.8ms the SHMC^8 acceptance rate reduces slightly to 99.8% while that of the SHMC^4 decreases to reach 88.2%. However, the HMC method acceptance rate is significantly decreased to 53.2%. Finally, when the time step reaches 4.8 ms, the acceptance rate reduces to 78.6% for the SHMC^8 and to 70.8% for the SHMC^4 which is an acceptable rate comparing to that obtained by the HMC method (less than 1%). Fig. 8 was plotted when the constant $c = 0.01$.

Despite the detailed mathematical formulation of the SHMC* this algorithm is easier to program. Albeit some extra memory (compared to the HMC algorithm) is needed for the extra parameters as well as the reweighting step during the execution of the program. However, with a good choice of the constant c, the SHMC* algorithms performs very well. Sweet et al. [51] proposed a method to optimize the SHMC algorithm. This method is based on finding the mean and variance of the difference between the shadow Hamiltonian and the Hamiltonian which will be useful to find optimal values for both c and δt. Moreover, the SHMC method successfully extended the time step upper bound where $\delta t_{max}^{SHMC} \geqslant 4.8$ ms (see Fig. 8) which allows large jumps during the search. Updating large structures with many updated parameters (more than 20

Please cite this article as: I. Boulkaibet, et al., Finite element model updating using the shadow hybrid Monte Carlo technique, Mech. Syst. Signal Process. (2014), http://dx.doi.org/10.1016/j.ymssp.2014.06.005

parameters) using the SHMC algorithms could be worth investigating since the parameters size in this approach has less effect (in term of stability and errors) than that of the HMC algorithm [26].

Different approaches have been made to improve the HMC efficiency. Neal [52] used the "reject" and "accept" windows to improve the acceptance rate of the HMC algorithm while Fischer et al. [53] introduced an extra parameter to generalize the HMC algorithm by enhancing sampling at low temperatures which is done by sampling from a mixed canonical ensemble. Combining the SHMC algorithm with some of these modifications mentioned above is considered in FEM updating and also will consider the differences between the above methods and other variations of the Hamiltonian Monte Carlo method.

9. Conclusion

This paper promotes the use of a Bayesian approach to finite element model updating. Using the Bayesian approach in this updating problem requires the evaluation of the posterior distribution function (PDF). Unfortunately due to the high dimensionality and complexity of updated structures, the posterior function is not available in analytical form. Traditionally numerical methods are then used to approximate such a function. The most popular of these are the Markov Chain Monte Carlo (MCMC) based sampling methods.

In this paper the Hybrid Monte Carlo (HMC) method is implemented to approximate the posterior distribution function. The results and limitations of the HMC on the FEM updating problem are highlighted. To overcome some of these limitations, we proposed the use of a modified version – which is based on a shadow Hamiltonian – called the Shadow HMC. The SHMC uses a modified Hamiltonian approximation to sample from the extended phase-space of the shadow Hamiltonian rather than the configuration space alone.

Two different real structures each with a given set of updating parameters are used as test cases for these sampling techniques.

The simulation results of the more complex structure indicate that some stiffness parameters are highly correlated and some of them are weakly correlated. Furthermore the updated parameters are not jointly Gaussian where some of these parameters have forms very close to a Gaussian distribution. Both methods provided good updates on the modal data and significantly reduced the FEM errors. In both simulation test cases the SHMC techniques gives better results than the HMC method.

In this study, the efficiency of these algorithms is shown where both methods converge fast for a given time step. However the SHMC method is more efficient than HMC where it provides good samples at larger time steps, which is not the case with the HMC method where the sampling rate decreases with an increased time step (the SHMC method extended the time step upper bound).

Future work will consider looking at the difference a two variable cost function makes in the updating of the finite element model. This could perhaps reveal certain subtleties in the application of the proposed sampling method.

References

[1] E. Oñate, Structural Analysis with the Finite Element Method, Linear Statics, Basis and Solids, Barcelona, CIMNE; London Springer, 2009.
[2] S.S. Rao, The Finite Element Method in Engineering, 4th ed. Elsevier Butterworth Heinemann, Burlington, 2004.
[3] M.I. Friswell, J.E. Mottershead, Finite Element Model Updating in Structural Dynamics, Kluwer, Academic Publishers, Dordrecht, Boston, 1995.
[4] T. Marwala, Finite Element Model Updating Using Computational Intelligence Techniques, Springer Verlag, London, UK, 2010.
[5] M. Baruch, I.Y. Barltzhack, Optimal weighted orthogonalization of measured modes, AIAA J. 16 (Issue 4) (1978) 346–351.
[6] A. Berman, E.J. Nagy, Improvement of large analytical model using test data, AIAA J. 21 (Issue 7) (1983) 1168–1173.
[7] H. H. hodaparast, Stochastic finite element model updating and its application in aeroelasticity (Ph.D. Thesis), Department of Civil Engineering, University of Liverpool, EThOS, UK, 2010.
[8] M. Link, 1999, Updating of analytical models, review of numerical procedures and application aspects, in: Proceedings of the Structural Dynamics Forum, Los Alamos, 2000.
[9] R.I. Levin, N.I.J. Lieven, Dynamic finite element model updating using simulated annealing and genetic algorithms, Mech. Syst. Signal Proc. 12 (1998) 91–120.
[10] A.A. Henriques, Efficient analysis of structural uncertainty using perturbation techniques, Eng. Struct. 30 (Issue 4) (2008) 990–1001.
[11] S.H. Cheung, J.L. Beck, Bayesian model updating using hybrid monte carlo simulation with application to structural dynamic models with many uncertain parameters, J. Eng. Mech. 135 (4) (2009) 243–255.
[12] I. Boulkaibet, T. Marwala, L. Mthembu, M.I. Friswell S. Adhikari, Sampling techniques in bayesian finite element model updating, Proceedings of the Society for Experimental Mechanics, 29, 2012 pp. 75–83.
[13] K.V. Yuen, Bayesian Methods for Structural Dynamics and Civil Engineering, Wiley, New York, 2010.
[14] M.D. McKay, R.J. Beckman, W.J. Conover, A comparison of three methods for selecting values of input variables in the analysis of output from a computer code, Techno-metrics 42 (Issue 1) (2000) 55–61.
[15] J.R. Koehler, A.B. Owen, Computer experiments, in: S. Ghosh, C.R. Rao (Eds.), Handbook of Statistics, 13, Elsevier Science B V, Amsterdam, 2000, pp. 261–308.
[16] W.K. Hastings, Monte Carlo sampling methods using Markov chains and their applications, Biometrika 57 (1) (1970) 97–109.
[17] N. Metropolis, A.W. Rosenbluth, M.N. Rosenbluth, A.H. Teller, E. Teller, Equations of state calculations by fast computing machines, J. Chem. Phys. 21 (1953) 1087–1092.
[18] S. Chib, E. Greenberg, Understanding the Metropolis–Hastings algorithm, Am. Stat. 49 (No. 4) (1995) 327–335.
[19] M. Girolami, B. Calderhead, Riemann manifold Langevin and Hamiltonian Monte Carlo methods, J. R. Stat. Soc. 73 (2) (2011) 123–214.
[20] T. Marwala, S. Sibisi, Finite element model updating using Bayesian approach, in: Proceedings of the International Modal Analysis Conference, Orlando, Florida, USA, 2005. ISBN: 0-912053-89-5.
[21] J. Ching, M. Muto, J.L. Beck, Structural model updating and health monitoring with incomplete modal data using Gibbs Sampler, Comput.-Aided Civil Infrastruct. Eng. 21 (4) (2006) 242–257.

Please cite this article as: I. Boulkaibet, et al., Finite element model updating using the shadow hybrid Monte Carlo technique, Mech. Syst. Signal Process. (2014), http://dx.doi.org/10.1016/j.ymssp.2014.06.005

[22] S. Geman, D. Geman, Stochastic relaxation Gibbs distributions and the Bayesian restoration of images, IEEE Trans. Pattern Anal. Mach. Intell. 6 (Issue 6) (1984) 721–741.
[23] J. Ching, Y.J. Chen, Transitional Markov chain Monte Carlo method for Bayesian model updating, model class selection, and model averaging, J. Eng. Mech. 133 (Issue 7) (2007) 816–832.
[24] M. Muto, J.L. Beck, Bayesian updating and Model Class Selection for hysteretic structural models using stochastic simulation, J. Vib. Control 14 (2008). (7-3).
[25] A. Beskos, N. Pillai, G. Roberts, J.M. Sanz-Serna, A. Stuart, Optimal tuning of the hybrid Monte Carlo algorithm, Bernoulli Soc. Math. Stat. Probabil. 19 (2013) 1501–1534.
[26] J.A. Izaguirre, S.S. Hampton, J. Comput, Shadow hybrid Monte Carlo: an efficient propagator in phase space of macromolecules, J. Comput. Phys. 200 (2004) 581–604.
[27] R.D. Skeel, D.J. Hardy, Practical construction of modified Hamiltonians, SIAM J. Sci. Comput. 23 (No 4) (2001) 1172–1188.
[28] R.D. Engle, R.D. Skeel, M. Drees, Monitoring energy drift with shadow Hamiltonians, J. Comput. Phys. 206 (2005) 432–452.
[29] I. Boulkaibet, L. Mthembu, T. Marwala, M.I. Friswell and S. Adhikari, Finite element model updating using the shadow hybrid Monte Carlo Technique, in: Conference Proceedings of the Society for Experimental Mechanics, 6 2013, pp. 489–498.
[30] D.J. Ewins, Modal Testing: Theory and Practice, Research Studies Press, Letchworth, 1984.
[31] C.M. Bishop, Pattern Recognition and Machine Learning, Springer-Verlag, New York, 2006.
[32] C.M. Bishop, Neural Networks for Pattern Recognition, Oxford University Press, Walton Street, Oxford, 1995.
[33] V.N. Vapnik, The Nature of Statistical Learning Theory, Springer Verlag, New York, 1995.
[34] J. Ching, S.S. Leu, Bayesian updating of reliability of civil infrastructure facilities based on condition-state data and fault-tree model, Reliabil. Eng. Syst. Saf. 94 (12) (2009) 1962–1974.
[35] R.M. Neal, Slice sampling, Ann. Stat. 31 (3) (2003) 705–767.
[36] K.M. Hanson, Markov Chain Monte Carlo posterior sampling with the Hamiltonian Method, Proc. SPIE 4322 (2001) 456–467.
[37] R.D. Skeel, P.F. Tupper, Mathematical issues in molecular dynamics, Banff Int. Res. Stn. Rep. (2005).
[38] J. Von Neumann, Various techniques used in connection with random digits, in: Monte Carlo Method, Applied Mathematics Series 12, National Bureau of Standards, Washington, D.C., 1951.
[39] G.S. Fishman, Monte Carlo: Concepts, Algorithms, and Applications, Springer Series in Operations Research, Springer-Verlag, New York, 2000.
[40] M. Creutz, Global Monte Carlo algorithms for many-fermion systems, Phys. Rev. D D 38 (1988) 1228–1238.
[41] A.D. Kennedy, B. Pendleton, Acceptances and autocorrelations in hybrid Monte Carlo, Nucl. Phys. B Proc. Suppl. 20 (1991) 118–121.
[42] E. Hairer, C. Lubich, G. Wanner, Geometric Numerical Integration, Structure-Preserving Algorithms for Ordinary Differential Equations, 2nd Edition, Springer Series in Computational Mathematics 31. Springer-Verlag, Berlin, 2006.
[43] E. Balmes, Predicted variability and differences between tests of a single structure, in: Proceedings of the International Modal Analysis Conference IMAC XVI, Santa Barbara, CA, 1998 pp.558–564.
[44] M. Degener, M. Hermes, Ground vibration test and finite element analysis of the GARTEUR SM-AG19 tested, Deutsche Forschungsanstalt für Luft und Raumfahrt e. V. Institut für Aeroelastik, IB 232-96J 08, 1996.
[45] J. Carvallo, B.N. Datta, A. Gupta and M. Lagadapati, A direct method for model updating with incomplete measured data and without spurious modes, Mechanical Systems and Signal Processing 21 (7), 2007, pp. 2715–2731.
[46] B.N. Datta, Finite element model updating, eigenstructure assignment and eigenvalue embedding techniques for vibrating systems, Mech. Syst. Signal Process. 16 (2002) 83–96.
[47] I. Guyon, A. Elisseeff, An introduction to variable and feature selection, J. Mach. Learn. Res. 3 (2003) 1157–1182.
[48] M. Link, M.I. Friswell, Generation of validated structural dynamic models—results of a benchmark study utilizing the GARTEUR SM-AG19 Testbed, Mech. Syst. Signal Process 17 (1) (2003) 9–20. (COST action special issue).
[49] C. Mares, J.E. Mottershead, M.I. Friswell, Selection and updating of parameters for the GARTEUR SM-AG19 Test-bed, International Conference on Noise and Vibration Engineering, September 2000.
[50] M. Link, M. Friswell, Working group 1: generation of validated structural dynamic models-results of a benchmark study utilising The GARTEUR SM-AG19 test-bed, Mech. Syst. Signal Process. 17 (1) (2003) 9–20.
[51] C. Sweet, S. Hampton, J. Izaguirre, Optimal Implementation of the Shadow Hybrid Monte Carlo Method, University of Notre Dame, Indiana, USA, 2006 (Tech. Rep. TR-2006-09).
[52] R.M. Neal, An improved acceptance procedure for the hybrid Monte Carlo algorithm, J. Comput. Phys. 111 (1994) 94–203.
[53] A. Fischer, F. Cordes, C. Schütte, Hybrid Monte Carlo with adaptive temperature in mixed-canonical ensemble: efficient conformational analysis of RNA, Comp. Phys. Commun. (1999) 37–39.

Please cite this article as: I. Boulkaibet, et al., Finite element model updating using the shadow hybrid Monte Carlo technique, Mech. Syst. Signal Process. (2014), http://dx.doi.org/10.1016/j.ymssp.2014.06.005